Manuscript prepared for Atmos. Chem. Phys.
with version 2014/09/16 7.15 Copernicus papers of the LaTeX class copernicus.cls.
Date: 9 November 2015

Can we explain the observed methane variability after the Mount Pinatubo eruption?

N. Bândă[1,2], M. Krol[3,4,1], M. van Weele[2], T. van Noije[2], P. Le Sager[2], and T. Röckmann[1]

[1]Institute for Marine and Atmospheric Research Utrecht, Utrecht University, Utrecht, The Netherlands
[2]Royal Netherlands Meteorological Institute (KNMI), De Bilt, The Netherlands
[3]Meteorology and Air Quality, Wageningen University and Research Center, Wageningen, The Netherlands
[4]Netherlands Institute for Space Research (SRON), Utrecht, The Netherlands

Correspondence to: N. Bândă (n.l.banda@uu.nl)

Abstract. The CH_4 growth rate in the atmosphere showed large variations after the Pinatubo eruption in June 1991. A decrease of more than 10 ppb yr^{-1} in the growth rate over the course of 1992 was reported and a partial recovery in the following year. Although several reasons have been proposed to explain the evolution of CH_4 after the eruption, their contributions to the observed variations are not yet resolved. CH_4 is removed from the atmosphere by the reaction with tropospheric OH, which in turn is produced by O_3 photolysis under UV radiation. The CH_4 removal after the Pinatubo eruption might have been affected by changes in tropospheric UV levels due to the presence of stratospheric SO_2 and sulfate aerosols, and due to enhanced ozone depletion on Pinatubo aerosols. The perturbed climate after the eruption also altered both sources and sinks of atmospheric CH_4. Furthermore, CH_4 concentrations were influenced by other factors of natural variability in that period, such as ENSO and biomass burning events. Emissions of CO, NO_X and NMVOCs also affected CH_4 concentrations indirectly by influencing tropospheric OH levels.

Potential drivers of CH_4 variability are investigated using the TM5 global chemistry model. The contribution that each driver had to the global CH_4 variability during the period 1990 to 1995 is quantified. We find that a decrease of 8-10 ppb yr^{-1} CH_4 is explained by a combination of the above processes. However, the timing of the minimum growth rate is found 6-9 months later than observed. The long-term decrease in CH_4 growth rate over the period 1990 to 1995 is well captured and can be attributed to an increase in OH concentrations over this time period. Potential uncertainties in our modelled CH_4 growth rate include emissions of CH_4 from wetlands, biomass burning emissions of CH_4 and other compounds, biogenic NMVOC and the sensitivity of OH to NMVOC emission changes. Two inventories are used for CH_4 emissions from wetlands, ORCHIDEE and

LPJ, to investigate the role of uncertainties in these emissions. Although the higher climate sensitivity of ORCHIDEE improves the simulated CH_4 growth rate change after Pinatubo, none of the two inventories properly captures the observed CH_4 variability in this period.

1 Introduction

Methane (CH_4) is the second most important anthropogenic greenhouse gas after carbon dioxide (CO_2). Its evolution in the atmosphere since the beginning of the record of continuous atmospheric CH_4 measurements in the 1980s is not fully understood, with large discrepancies between bottom-up and top-down estimates of CH_4 sources and sinks (Kirschke et al., 2013). One of the events that affected CH_4 concentrations was the eruption of Mt. Pinatubo on 15 June 1991, the largest eruption in the last century. The eruption caused perturbations to climate and photochemistry for a few years afterwards. We investigate here the sensitivity of CH_4 concentrations to these perturbations, and our ability to explain the observed CH_4 variations in the atmosphere in the early 1990s.

After a stable CH_4 growth rate of 10 to 13 $\mathrm{ppb\,yr^{-1}}$ in the late 1980s, the growth rate showed large fluctuations in the early 1990s. An increased CH_4 growth rate of about 17 $\mathrm{ppb\,yr^{-1}}$ was registered by the NOAA network in 1991, followed by a strong decline in the growth rate during the next year, with values reaching nearly zero (Dlugokencky et al., 1994). The growth rate recovered to 6 $\mathrm{ppb\,yr^{-1}}$ in 1993. Processes driving these variations could be related to either the CH_4 sources or the CH_4 sinks.

CH_4 is emitted to the atmosphere from anthropogenic activities (fossil fuel production, agriculture and waste treatment), biomass burning, and from natural sources (wetlands, geological activity, termites). The main sink of atmospheric CH_4 is the reaction with the hydroxyl radical (OH) in the troposphere, which removes about 80% of the CH_4. Other removal processes are soil uptake, reactions with chlorine (Cl) in both the troposphere and stratosphere, and reactions with OH and excited oxygen ($O(^1D)$) atoms in the stratosphere. Tropospheric OH is produced by the photolysis of ozone (O_3) at wavelengths of 280-320 nm, followed by the reaction of $O(^1D)$ with water vapour. Therefore the abundance of OH in the troposphere is sensitive both to the amount of incoming UV radiation and to the water vapour abundance. Tropospheric OH also reacts with other atmospheric compounds such as carbon monoxide (CO) and non-methane volatile organic compounds (NMVOC), and is recycled in the presence of nitrogen oxides (NO_X). Thus, changes in the emissions of NO_X, CO and NMVOCs also affect the OH abundance (Lelieveld et al., 2002).

Interannual variations in both the sources and sinks of CH_4 occurred in the early 1990s. In part, these can be related to the Pinatubo eruption, which caused a decrease in tropospheric temperatures of about 0.5°C globally in the two following years (McCormick et al., 1995). The global cooling most likely resulted in a decrease in the CH_4 emission rates from wetlands. Methane emissions from wetlands might have also been inhibited by the deposition of volcanic sulfur from the eruption (Gauci et al., 2008).

The removal of CH_4 by OH is a temperature-dependent reaction which was also affected by the temperature decrease after the eruption. OH production would have further responded to the decrease in water vapour associated with the temperature reduction (Soden et al., 2002). The climate anomaly after Pinatubo might have affected natural emissions of other species as well, such as NMVOC emissions from vegetation, which may in turn have caused changes in OH and thus the CH_4 sink. Changes in UV radiation due to stratospheric aerosols and stratospheric O_3 anomalies would have also affected the removal of CH_4 by OH in the post-Pinatubo years (Dlugokencky et al., 1996; Bekki et al., 1994; Bândă et al., 2014, from here on referred to as B14). Stratospheric O_3 variations in this period were caused by heterogeneous removal on volcanic aerosol particles, by atmospheric transport changes due to the eruption, and by other factors of natural variability (Telford et al., 2009; Bekki and Pyle, 1994).

Another potential effect of the eruption on the CH_4 budget is altered transport between the troposphere and the stratosphere due to the stratospheric warming by volcanic particles (Schauffler and Daniel, 1994). CH_4 concentrations in the post-Pinatubo period were also affected by natural variability not related to Pinatubo, such as the 11-year solar cycle, the El-Niño Southern Oscillation (ENSO) cycle and biomass burning events. Significant reductions in the anthropogenic emissions from gas production and distribution in the Former Soviet Union (FSU) might have occurred in this period (Law and Nisbet, 1996). However, gaps in reporting make the magnitude and timing of these reductions quite uncertain.

Previous bottom-up studies quantified the impact of individual processes on the CH_4 abundance, without attempting to solve the whole CH_4 budget. Bekki and Law (1997) found compensating effects of temperature on the CH_4 emissions and the CH_4 removal by OH on a global scale. Dlugokencky et al. (1996) showed that the increase in both CH_4 and CO mixing ratios in late 1991 and early 1992 could be related to a decrease in OH due to UV scattering by stratospheric aerosols and UV absorption by sulfur dioxide (SO_2) from the eruption. A more recent estimate from B14 finds a decrease of 11.2 and 6.6 Tg, respectively, in the CH_4 removal in the first and second years following the eruption due to stratospheric sulfur. The above decreases in CH_4 removal translate into corresponding increases of 4 and 2 $\mathrm{ppb\,yr^{-1}}$, respectively, in the CH_4 growth rate. Here and in the remainder of the paper, we use the ratio of 2.78 Tg/ppb reported by the IPCC (Denman et al., 2007) to convert from CH_4 burden changes to growth rate variations. Using a two-dimensional model, Bekki et al. (1994) attributed half of the decrease in CH_4 and CO growth rates in 1992 to stratospheric O_3 depletion. Additionally, Dlugokencky et al. (1994) and Law and Nisbet (1996) estimated that a decrease in the gas leak emissions from the FSU could be in the order of 15 $\mathrm{Tg\,yr^{-1}}$, and would also explain part of the observed decrease in the CH_4 growth rate in 1992. Using a 4-box model, Schauffler and Daniel (1994) found that an increase in the exchange rate between stratosphere and troposphere due to volcanic aerosol heating can cause lower CH_4 concentrations in the troposphere.

Prior attempts to explain the CH_4 variability in this period include inverse modelling studies and a column model study. The inverse modelling studies of Bousquet et al. (2006) and Wang et al. (2004) (B06 and W04 from here on, respectively) find a positive anomaly in the CH_4 flux to the atmosphere in 1991, and a negative anomaly in 1992, with a difference of about 30 Tg between the two years. Both studies find a significant contribution from wetland emissions to this anomaly and a small contribution from biomass burning. However, the two studies use OH variations of opposite sign. The OH fields in B06 are determined by methyl chloroform inversions, showing a reduced OH sink of CH_4 of about 30 $\mathrm{Tg\,yr^{-1}}$ over the period 1991 to 1993 compared to 1990. To close the CH_4 budget, their anthropogenic and wetland CH_4 emissions also show pronounced decreases. When using both CH_4 and methyl chloroform to constrain OH, Pison et al. (2013) found a more moderate OH variability. In W04, OH is parameterised based on chemical and meteorological parameters with coefficients determined from 3D model simulations. W04 find an increase of about 5% in OH from 1991 to 1993 due to stratospheric O_3 depletion. Stratospheric aerosols from the eruption are, however, not included as a parameter in their calculation. Our previous column model study (Bândă et al., 2013) supports a decrease in OH in the first year after the eruption due to aerosols, temperature and water vapour changes, and a subsequent decrease due to stratospheric O_3 depletion. In that study we found that the stratospheric O_3 depletion together with changes in anthropogenic emissions could explain a 12 $\mathrm{ppb\,yr^{-1}}$ decrease in 1993 compared to 1991. However, the one-dimensional model was unable to capture the strong CH_4 decrease in 1992.

In the present study, we quantify the combined impact of the drivers of CH_4 variability described above in the early 1990s using the global chemistry and transport model TM5 and we identify the potential gaps in our understanding of the CH_4 budget. For the first time, all the known processes that could have significantly contributed to the CH_4 variations in the early 1990s are included in a modelling study.

The manuscript is structured as follows. A description of the TM5 model is presented in Section 2.1 and of the simulation setup in Section 2.2. Section 2.3 describes the drivers that have been considered to explain the observed CH_4 variability, and Section 3.1 presents their impact on the simulated CH_4 budget. The unexplained CH_4 variability is shown in Section 3.2, and possible reasons for mismatch between the model and observations are discussed in Section 4. Conclusions are drawn in Section 5.

2 Method

2.1 Model description

The TM5 global chemistry and transport model (Huijnen et al., 2010; Williams et al., 2012; van Noije et al., 2014) was used to simulate the chemical composition of the atmosphere during the period 1990 to 1995. The model was run on 60 hybrid sigma-pressure vertical levels and at a horizontal resolution of 3° x 2° (longitude x latitude) globally, except for the polar region, where a reduced grid was used for advection in the zonal direction. The model was driven by meteorological fields from the ECMWF ERA-Interim reanalysis (Dee et al., 2011). The gas-phase chemistry scheme is based on a modified version of the carbon bond mechanism 4 (Houweling et al., 1998). Photolysis frequencies are calculated by the on-line parameterisation scheme based on Williams et al. (2006). To account for missing O_3 chemistry in the stratosphere, O_3 is nudged to the multi sensor reanalysis data (MSR; van der A et al., 2010) above the 45 hPa level in the tropics (30°S-30°N) and above the 90 hPa level in the extra-tropics. CH_4 is also nudged above these pressure levels to climatological values from Grooß and Russell III (2005) to compensate for possible errors in stratospheric chemistry, specifically the loss of CH_4 by OH, Cl and $O(^1D)$. The performance of TM5 in simulating atmospheric chemistry is presented in Huijnen et al. (2010) and van Noije et al. (2014). The conclusions of these studies remain valid with the current setup.

The modal scheme M7 (Vignati et al., 2004; Aan de Brugh et al., 2011) is used to simulate aerosol microphysics. M7 simulates the following aerosol types: sulfate (SO_4), black carbon (BC), organic carbon (OC), sea salt and mineral dust. In addition, TM5 calculates ammonium and nitrate partitioning between gas phase and aerosols using the Equilibrium Simplified Aerosol Model (EQSAM; Metzger et al., 2002), and accounts for methyl sulfonic acid (MSA). The aerosols are coupled to the radiative transfer scheme that is used to calculate photolysis frequencies. Some adjustments to the M7 default setup have been applied in order to realistically simulate stratospheric volcanic aerosols, as described in B14. This setup has been used in the aforementioned paper to model SO_2 and sulfate aerosols from the Pinatubo eruption, and to infer their effect on photolysis frequencies.

Here we use the new massively parallel model version TM5-mp. The new MPI parallelisation does not influence the model results, but brings a significant speedup of the model runs by allowing us to use more computing cores more efficiently. A few additional updates have been incorporated in the model compared to the version used in B14. Convective fluxes used for tracer transport are now read from the ERA-Interim input data, instead of calculating them with the Tiedtke scheme (Tiedtke, 1989). Heterogeneous removal of N_2O_5 on aerosol and cloud particles was updated according to Huijnen et al. (2014). The CH_4 surface nudging timescale has also been adjusted. We now use a nudging timescale of 10 days instead of 3 days in B14. By comparing the budget terms and concentrations of simulations with the different nudging timescales, we find that both nudging timescales give a similar performance in simulating the CH_4 concentrations and inter-annual variability (IAV).

Although similar global nudging values are found for the two simulations, the local nudging amount is 2 to 3 times larger using a 3-day nudging. Therefore we find that a 10-days nudging timescale is more appropriate for inferring CH_4 budget mismatches based on monthly observations, allowing for synoptic-scale variability in CH_4 concentrations (Dentener et al., 2003). Finally, some of the emission inventories used here differ from the ones used in B14, and are described below. We verified that the model updates did not cause any significant differences in modelled SO_2 and stratospheric aerosols compared to the results presented in B14.

Table 1 lists the CH_4 source and sink categories, the inventories used, and their yearly global mean and variability over the period 1990 to 1995. Two inventories for CH_4 emissions from wetlands are employed to investigate the uncertainty in these emissions. We use the ORCHIDEE emissions from the WETCHIMP intercomparison project (Wania et al., 2013) and LPJ emissions from the Hydrogen, Methane and Nitrous oxide (HYMN) project (Spahni et al., 2011). Other natural CH_4 monthly emissions from wild animals and termites were also used as compiled in HYMN. CH_4 soil removal rates from the LPJ inventory were applied. Anthropogenic emissions of CH_4, CO, NO_X, NMVOC, SO_2 and ammonia (NH_3) were taken from the EDGAR4.2 inventory, except for transport sector, for which EDGAR4.1 was used. Decadal anthropogenic emissions of BC and OC were taken from the historical AR5 emission inventory (Lamarque et al., 2010). Biomass burning emissions of CH_4, CO, NMVOC, NO_X, SO_2 and NH_3 are used from the RETRO inventory (Schultz et al., 2008). Production of NO_X by lightning and emissions of dimethyl sulfide (DMS), sea salt and dust are calculated online (Huijnen et al., 2010; Vignati et al., 2010; van Noije et al., 2014). Monthly biogenic emissions of CO, NH_3 and NMVOC were taken from the MEGAN inventory (Sindelarova et al., 2014). Climatological emissions from the MACC inventory are used for continuous volcanic SO_2 (Andres and Kasgnoc, 1998) and biogenic NO_X emissions.

2.2 Simulation setup

We designed a series of simulations with the aim to quantify the impact of specific processes on the tropospheric CH_4 concentrations. The difference between two simulations, one including, and one excluding a specific driver, is used to quantify the effect of that driver. For instance, we calculate the effect of IAV in meteorology on tropospheric CH_4 as the difference of a simulation that includes varying meteorological fields and a simulation that fixes meteorological fields to 1990 values. Two sets of simulations were performed for seven drivers of CH_4 variability for the period 1990 to 1995, as outlined in Table 2.

As described in B14, we use a two-step setup to simulate realistic CH_4 concentrations. In a first simulation of the 'Base1' and 'Base2' scenarios, in which all drivers of CH_4 variability are included, we nudge CH_4 mixing ratios in the lowest 2 km of the model towards measured mixing ratios from background sites. This allows us to account for uncertainties in sources and sinks of CH_4 and to avoid a long-term drift of mixing ratios compared to observations. This setup is particularly important for the second simulation set using the lower LPJ wetland emissions, where nearly 100 Tg yr^{-1} additional source or reduced sink is needed to close the CH_4 budget. The nudging is performed as follows. The North-South gradient in CH_4 mixing ratio is reconstructed by interpolating the measured CH_4 monthly mean mixing ratios at the background stations South Pole, Cape Grim, Mauna Loa, Niwot Ridge, Barrow, and Alert. In this way a realistic zonal mean CH_4 distribution is obtained from the observations, which is then compared to the modelled concentrations at the dateline. The concentrations in the whole zonal band are then adjusted based on this comparison. The amount of CH_4 needed to compensate for the difference between the model and observation-based North-South gradient in CH_4 is stored on a monthly basis for each 10-degree latitude band. In the second step, CH_4 is no longer constrained by observations, but instead the nudging amount calculated in the first step is applied as an emission in all scenarios. In B14 we used this nudging to scale the CH_4 emissions in each 10-degree latitude band. In these simulations, we observed slight time shifts in the derived CH_4 growth rates in the second step compared to the first step. To obtain an almost perfect match between the simulated CH_4 concentrations of the two steps, in the present study we apply the nudging homogeneously over the latitude band and in the lowest 2 km from the surface. This two-step setup enables us to model realistic CH_4 concentrations, and at the same time allowing them to respond to changes in emissions or photochemistry. The nudging term that is needed to force the 'Base1' and 'Base2' simulations to background atmospheric observations indicates in which latitude bands sources and sinks are unbalanced when all drivers of CH_4 variability are included. These mismatches will be further analysed in Section 3.2. Validation results for this two-step setup are shown in Appendix A.

The first simulation set (Set I in Table 2) uses the ORCHIDEE inventory for natural CH_4 emissions from wetlands, while the second set of simulations uses the LPJ inventory. The 'Base1' simulation from the first simulation set accounts for all drivers of CH_4 IAV in the model, including modelled stratospheric sulfur, varying amounts of stratospheric O_3, ERA-Interim fields for temperature and humidity, and emission variations of CH_4 and other species. Emission of SO_2 in the stratosphere by the Pinatubo eruption of 18.5 Tg SO_2 were considered, and the SO_2 subsequently reacts with OH to form aerosols. In the other simulations, we fix different variables in the model to investigate their effect on CH_4 concentrations. In all simulations except for the 'Base1' simulation, we removed the effects of Pinatubo SO_2 and sulfate, because using different meteorology or O_3 column might lead to different SO_2 and aerosol fields. By using this setup we minimise the nonlinearities between drivers of CH_4 variability. In 'FixMeteo1' and 'FixOzone1', we additionally used the meteorology and, respectively, the stratospheric O_3 of the year 1990 for the whole length of the simulation. In the 'FixWetl1' simulation we used constant CH_4 emissions from wetlands and CH_4 soil uptake rates from the year 1990. Simulation 'FixEmis' used anthropogenic and biomass burning emissions of CH_4 and other species from the year 1990. Biogenic emissions of CO, NMVOC and NO_X are also fixed to 1990 in 'FixEmis'. Finally, to infer the combined effect of all seven drivers of CH_4

variability, the simulation ‘FixAll1’ is performed, where all drivers of variability are fixed to 1990 values. This allows us to quantify the possible effect of nonlinearities, as discussed in Appendix B.

To test the impact of using a different inventory for CH_4 emissions from wetlands, a second set of simulations (Set II in Table 2) is performed using LPJ emissions. The second set of simulations consists of simulations ‘Base2’, ‘NoPinS2’ and ‘FixWetl2’, which are equivalent to the ‘Base1’, ‘NoPinS1’ and ‘FixWetl1’, respectively, of the first set. The ‘Base2’ simulation is similar to the ‘PinS’ simulation in B14, extended for three more years. The LPJ emissions and soil uptake rates from the year 1990 are used in ‘FixWetl2’ throughout the simulation.

2.3 Drivers of CH_4 variability

In this section we present the drivers of CH_4 variability in our model. The factors that affect the CH_4 sinks are stratospheric sulfur, stratospheric O_3, changes in meteorology, and emissions of CO and NMVOC. The CH_4 emissions for different sectors are also presented. We show model results for sulfate aerosol, while for other drivers of CH_4 variability we give a quantitative description of the input data. Their impact on the CH_4 concentration is analysed in Section 3.1.

The main drivers of CH_4 variability in our model for the period 1990 to 1995 are shown in Figure 1. All variables have been averaged with a 12-month running mean to remove the seasonal cycle. The globally averaged stratospheric aerosol optical depth (AOD) is shown in Figure 1a. The simulated AOD values were validated against measurements in B14. A global maximum AOD of 0.16 is simulated in early 1992. The aerosols remained in the stratosphere for a few years, with the AOD returning to pre-eruption levels towards the end of 1994.

Figure 1b presents the average stratospheric O_3 above 150 hPa between 60°S-60°N from the MSR data set (van der A et al., 2010). High-latitude O_3 anomalies are not taken into account here because the CH_4 is mainly oxidised in the tropics and at mid-latitudes during summer. A number of processes caused variations in stratospheric O_3 in the period 1990 to 1995. The 11-year cycle in solar radiation determined an overall decrease of 2.5% (6 Dobson Units) in the O_3 column over this period. The quasi-biennial oscillation (QBO) in stratospheric winds caused an additional IAV of about 1% (2 DU). In addition to these natural cycles, enhanced O_3 depletion occurred in 1992 to 1994 due to dynamical changes and heterogeneous chemistry associated with the presence of Pinatubo sulfate particles in the stratosphere (Telford et al., 2009; Aquila et al., 2013). This caused a 3.5% (8 DU) decrease in stratospheric O_3 from 1991 to early 1993, with largest perturbations observed at northern mid-latitudes. A smaller decrease of about 4 DU is found in the tropics (Shepherd et al., 2014). The effect of observed O_3 variations on CH_4 concentrations is investigated in Section 3.1. We do not separate in this study the effect of Pinatubo on stratospheric O_3 from other factors of O_3 variability.

A global-scale decrease in surface temperature was registered in 1992 caused by the decrease in surface shortwave radiation due to the volcanic aerosols. The effect of the eruption was partly counteracted by the 1992-1993 El-Niño (McCormick et al., 1995). In our ERA-Interim input data we find a global mean temperature decrease of 0.5°C in the free troposphere and of 0.3°C at the surface between 1990 and 1992, followed by a temperature recovery in 1994 (Figure 1c). The temperature decrease was associated with a 3% decrease in tropospheric water vapour. Other meteorological changes in this period, such as dynamics or cloudiness, might have also affected the stratosphere-troposphere exchange of CH_4 and the CH_4 removal by OH. Although these other meteorological parameters are not presented in this section, their potential effects on CH_4 are included when comparing the 'NoPinS' and 'FixMeteo' simulations.

Variability in emissions of chemical species might have determined changes in OH concentrations. Global CO and NO_X emissions have a similar evolution over the period 1990 to 1996, mainly driven by variations in biomass burning (Figure 1d). A large biomass burning event in 1992 leads to an increase of 100 Tg CO yr^{-1} in CO emissions and of 1.5 Tg NO_X yr^{-1} in 1992, and a decrease of similar magnitude one year afterwards. The NO_X emissions remain relatively constant throughout the rest of the period, while CO emissions decrease by about 50 Tg between 1990 and 1996. Biogenic emissions of NMVOC can also influence CH_4 concentrations indirectly through their reaction with OH. Isoprene, the NMVOC species with the largest emission rate in the atmosphere, is mainly produced by plants. Biogenic isoprene emissions are sensitive to changes in temperature, precipitation and radiation, and were likely affected by the Pinatubo eruption (Telford et al., 2010; Wilton et al., 2011). Global emissions of isoprene, shown in Figure 1e, given by the MEGAN inventory are 640-660 Tg yr^{-1} during 1990 and 1991. Over the coarse of 1992, the isoprene emissions decrease by about 70 Tg yr^{-1}, remaining at about 580-600 Tg yr^{-1} throughout the simulations period.

Changes in the main CH_4 emission categories are presented in Figure 1f-h. Inter-annual variability in total CH_4 emissions is dominated by emissions from wetlands and biomass burning. Both the LPJ and ORCHIDEE inventories show decreased CH_4 emissions from wetlands in 1991-1993. However, the exact timing and magnitude varies considerably between the two inventories, as well as the global emission amount and IAV. The ORCHIDEE inventory finds on average 266 Tg yr^{-1} CH_4 global emissions from wetlands, with interannual variability of 11.9 Tg yr^{-1} (see Table 1). The largest anomaly in this period is found after the Pinatubo eruption, with a decrease of 30 Tg yr^{-1} between the time of the eruption and one year afterwards. The LPJ inventory shows global wetland emissions of 166 Tg yr^{-1} with IAV of 2.6 Tg yr^{-1}. A decrease of 8 Tg yr^{-1} in CH_4 emissions from wetlands is found by LPJ during the year of the eruption, and a recovery starting from early 1992. Wetland extent has been shown to be important for simulating the IAV in wetland emissions, and might be a reason for the large differences between the two models (Ringeval et al., 2010; Spahni et al., 2011). ORCHIDEE simulates wetland extent interactively through the coupling to the TOPMODEL hydrology, while LPJ uses fixed wetland extent. The ORCHIDEE global emissions have been shown to be larger than those of other models from the WETCHIMP intercomparison study, having a high sensitivity to changes in CO_2, temperature and precipitation (Melton et al., 2013).

We used in our simulations the biomass burning emissions of CH_4 reported by the RETRO inventory, which amount to a global mean of 19.7 $\mathrm{Tg\,yr^{-1}}$ over this period, with an IAV of 2.6 $\mathrm{Tg\,yr^{-1}}$ and higher emissions in the years 1991, 1992 and 1994. The IAV in RETRO is determined from national fire reports, and from climate, soil moisture and carbon pool data used in the regional fire model Reg-FIRM (Schultz et al., 2008). Global anthropogenic emissions were quite stable at 256 to 261 $\mathrm{Tg\,yr^{-1}}$ during 1990 to 1995, according our input date based on EDGAR 4.2 and REAS 1 emission inventories, with an IAV of 1.2 $\mathrm{Tg\,yr^{-1}}$ and an increase towards the end of the period. More significant changes occurred at a regional level, with an overall increase in emissions in South-East Asia, and a decrease in Europe, North America and the FSU in this time period. Note, however, that inverse modelling studies report significantly higher total anthropogenic CH_4 emissions for this time period than the bottom-up inventories, exceeding 350 $\mathrm{Tg\,yr^{-1}}$ (Kirschke et al., 2013; Pison et al., 2013).

3 Results

3.1 Explained CH_4 variability

By taking differences between the budget terms of the simulations in Table 2 we are able to infer the effect of each driver of CH_4 variability described above. Figure 2 shows zonally averaged differences in CH_4 sources and sinks between the different simulations, vertically integrated over the troposphere. These differences are integrated up to a tropopause level defined here as a function of latitude, as recommended in Lawrence et al. (2001).

Absorption of UV radiation by volcanic SO_2 and UV scattering by sulfate aerosol are both included in the 'Base1' simulation, and lead to a decrease of UV radiation entering the troposphere. As shown in B14, the effect of stratospheric aerosols on global CH_4 is dominating and longer lived in comparison to the effect of SO_2 absorption. A decrease in the CH_4 sink is depicted in Figure 2a due to stratospheric sulfur, calculated as the difference between the 'Base1' and 'NoPinS1' simulations. The impact of stratospheric sulfur is strongest in the months after the eruption in the tropical region, with decreases in the zonal mean CH_4 sink of 2 to 5 $\mathrm{mg\,m^{-2}\,month^{-1}}$. Starting from 1993, the difference in the CH_4 sink due to stratospheric sulfur decreases below 1 $\mathrm{mg\,m^{-2}\,month^{-1}}$ globally.

Stratospheric O_3 decreased in the tropical region in 1991 to 1995 compared to 1990. A slight increase in stratospheric O_3 was observed in 1991 in the southern mid-latitudes because of an increase in the strength of the Brewer-Dobson circulation due to stratospheric heating by Pinatubo aerosols (Aquila et al., 2013). Figure 2b shows that these stratospheric O_3 changes led to variations in the OH sink of CH_4 between -5 and +10 $\mathrm{mg\,m^{-2}\,month^{-1}}$ in the period 1991 to 1996. Decreases in the CH_4 sink of up to 5 $\mathrm{mg\,m^{-2}\,month^{-1}}$ are modelled in 1991 in the extra-tropics, compensated by increases of similar magnitude in the equatorial region. From 1992 to 1996, reduced stratospheric O_3 levels caused increases in the CH_4 sink in the equatorial band, the northern tropics and part of the northern mid-latitudes. An increase in the CH_4 sink of more than 5 mg m^{-2} month^{-1} is modelled in the northern tropics in the summers of 1993, 1994 and 1995.

The decrease in temperature and water vapour following the eruption led to a decrease in both OH production and the rate of reaction between OH and CH_4. Our model results show that variations in meteorology caused decreases in the CH_4 sink of 2 to 10 mg m^{-2} month^{-1} in the northern tropical region during September 1991 to March 1993, and in the northern mid-latitudes during the summers of 1992 and 1993 (Figure 2c).

Variations in emissions of other species indirectly affect CH_4 concentrations through the CH_4 sink. On the one hand, CO and NMVOC emissions decrease OH concentrations because of their reaction with OH. Recycling of OH, on the other hand, increases due to NO_X emissions. Anthropogenic activity and biomass burning events lead to emissions of all these compounds. In addition, the difference between ‘NoPinS’ and ‘FixEmis’ also includes changes in biogenic emissions of CO and NMVOC that are sensitive to climate variations (Sindelarova et al., 2014). The overall effect on OH is determined by the relative increases in total emissions of CO and NMVOC compared to total NO_X emissions (Dalsøren and Isaksen, 2006). The OH variability due to changes in emissions is shown in Figure 2d. Particularly large decreases in emissions of CO from biomass burning and in biogenic NMVOC emissions in our input data occurred between 1992 and 1993, leading to an increase of 3 to 5 mg m^{-2} month^{-1} in the CH_4 sink.

Figure 2e and 2f show differences in wetland emission strength with respect to the year 1990 for the ORCHIDEE and LPJ emission inventories. These emission differences are often larger that those found for the CH_4 sink, but they are of shorter duration and more localised. The most striking difference between the CH_4 emission variations in the LPJ and in the ORCHIDEE inventories is their magnitude. While the magnitude of LPJ differences compared to 1990 have values mostly between -10 and 10 mg m^{-2} month^{-1}, the ORCHIDEE differences often exceed 20 mg m^{-2} month^{-1}. Both inventories show a decrease in emissions in the tropics and in the Northern Hemisphere in late 1991 and early 1992. The strength and the duration of the decrease differs between the two inventories. In the equatorial region, ORCHIDEE gives decreases that often surpass 20 mg m^{-2} month^{-1} from 1992 to 1995. LPJ reports decreased emissions in the equatorial region in the second half of 1991 and first half of 1992. This period is followed by alternating short periods of increased and decreased emissions near the equator until 1995. Both inventories give some increases in emissions in the subtropics throughout the period and a strong increase in emissions throughout the tropics in the second half of 1995 and beginning of 1996. In the northern mid- and high-latitudes, decreases of 2 to 5 mg m^{-2} month^{-1} are maintained from the second half of 1991 to mid-1993 in LPJ. In ORCHIDEE, CH_4 emissions decrease by up to 20 mg m^{-2} month^{-1} in the first half of 1992, but are compensated by increases of similar magnitude in the second half of 1992. Increased emissions are reported by ORCHIDEE in this region every summer from 1993 to 1995.

Variations in emissions other than wetlands also cause significant changes in the CH_4 budget. The CH_4 emissions are affected by variations in biomass burning and anthropogenic activity (Figure 2g). Anthropogenic emissions in the northern mid-latitudes show a gradual decrease of up to 20 $\mathrm{mg\,m^{-2}\,month^{-1}}$ from 1990 to 1996. This decrease is compensated by an increase in anthropogenic emissions in the tropical region, with values reaching 5 to 10 $\mathrm{mg\,m^{-2}\,month^{-1}}$ between 15-30°N. Enhanced biomass burning emissions are also found close to the equator in the autumn of the years 1991, 1992, and 1994.

The modelled growth rate variations caused by the changes in CH_4 sources and sinks described above are depicted in Figure 3. A 12-month running mean was applied to all the growth rate variations, to remove seasonal effects. The black line shows the cumulative effect of these processes on the CH_4 growth rate, representing the combined effect of all considered drivers of variability on the global CH_4 growth rate, which we will refer to as the 'explained' CH_4 growth rate. We assume here additivity between the changes in CH_4 growth rate caused by the different drivers. The effect of nonlinearities is discussed in Appendix B. Figures 3a and 3b show the two cases in which the ORCHIDEE and the LPJ inventory, respectively, are used to represent the effect of IAV in wetland CH_4 emissions. In early 1991 the CH_4 growth rate remains within 2 $\mathrm{ppb\,yr^{-1}}$ of that in 1990. Values of more than 10 $\mathrm{ppb\,yr^{-1}}$ are found in 1990-1991 (see Figure 7) due to relatively high emissions from all source categories of CH_4. The relatively large ozone column values in these years, together with large emissions of CO and NMVOC, lead to a reduced CH_4 sink in 1990 and 1991. During 1991 the explained CH_4 growth rate remains stable or shows a moderate increase depending on whether the ORCHIDEE or, respectively, the LPJ inventory is used. The explained CH_4 growth rate decreases afterwards by 9-10 $\mathrm{ppb\,yr^{-1}}$ in both cases, partly due to a decrease in wetland emissions. While CH_4 emissions from wetlands gradually recover, a combination of other processes leads to a continued decrease in CH_4 growth rate until 1993. The processes contributing to the decrease in the explained CH_4 growth rate in the second half of 1992 and early 1993 are stratospheric O_3 depletion, a recovery of stratospheric aerosols towards background levels, and changes in other emissions than CH_4 emissions from wetlands. The former effect includes a decrease in CH_4 emissions from biomass burning of 4-5 $\mathrm{Tg\,yr^{-1}}$ between 1992 and 1993, and a 2 $\mathrm{Tg\,yr^{-1}}$ decrease in anthropogenic emissions. This would lead to a combined decrease of 6-7 $\mathrm{Tg\,yr^{-1}}$, or 2 $\mathrm{ppb\,yr^{-1}}$. A decrease in isoprene emissions of 60 $\mathrm{Tg\,yr^{-1}}$ and a decrease of 50 $\mathrm{Tg\,yr^{-1}}$ in CO emissions also occur over this period. They cause an increase in the CH_4 removal and lead to a decrease of 6 $\mathrm{ppb\,yr^{-1}}$ in 'FixEmis1' compared to 'NoPinS1'. The overall effect remains stable at -6 to -7 $\mathrm{ppb\,yr^{-1}}$ from mid 1993 to spring 1994.

Although the evolution of the explained CH_4 growth rate shows similar features when using the two wetland emission inventories, some significant differences occur. First, the more pronounced decrease in CH_4 emissions in ORCHIDEE in 1991 compensates the concurrent decrease in the CH_4 sink due to stratospheric aerosols and meteorological changes, leading to a stable CH_4 growth rate during 1991. The decrease in LPJ emissions in 1991 is much smaller, resulting in a 3.5 $\mathrm{ppb\,yr^{-1}}$

increase in CH_4 growth rate in the second half of 1991. The decrease in the explained CH_4 growth rate that follows in 1992 starts about half a year later when using LPJ emissions than when using ORCHIDEE. The 8 ppb yr^{-1} decrease in the growth rate obtained with ORCHIDEE in late 1991 and early 1992 causes an earlier decrease in the overall growth rate. The minimum CH_4 growth rate also occurs in about three months earlier with ORCHIDEE than with LPJ. Finally, an additional 3 ppb yr^{-1} growth rate decrease occurs during 1994 with ORCHIDEE, while LPJ gives a stable CH_4 growth rate between mid-1993 and mid-1995.

Our explained CH_4 growth rates are compared to observations in Figure 4. Two estimates for the observed global mean growth rate are shown. The first estimate is calculated from the NOAA GLOBALVIEW-CH4 (2009) marine boundary layer zonal mean CH_4 concentrations. The second estimate, 'Background5', is taken from the CH_4 background data used for nudging the model, based on measurements from five stations (see Section 2.2). The other CH_4 growth rate curves in Figure 4 are the same as the black lines in Figure 3, representing the explained growth rate differences with respect to 1990. In order to obtain the variability with respect to the year 1990 from the observations, the 1990 CH_4 growth rates have been subtracted from both observation timeseries (see absolute growth rate values in Figure 7). A running mean of 12 months was further applied to remove seasonal effects. The explained CH_4 growth rate variability shows differences of -1.0 to 2.5 ppb yr^{-1} in 1991 with respect to 1990, which falls in between the two observational estimates of 3 ppb yr^{-1} for GLOBALVIEW-CH4, and -1.5 ppb yr^{-1} for 'Background5'. The model gives an increase of 3.5 ppb yr^{-1} over the course of 1991 when using LPJ, while using ORCHIDEE we find a decrease of 1 ppb yr^{-1}. The observations from GLOBALVIEW show an increase in the CH_4 growth rate in the first half of 1991 and a decrease in the second half, while the 'Background5' growth rate decreases throughout the year 1991. A continued decrease in the CH_4 growth rate is found in observations in 1992, reaching -10 ppb yr^{-1} in autumn 1992. The explained growth rate also decreases compared to 1990 when using ORCHIDEE emissions, reaching -8 ppb yr^{-1} about half a year later than the observations. With LPJ emissions, the decrease in the CH_4 growth rate occurs between spring 1992 and summer 1993, reaching -6 ppb yr^{-1}. The observations show a further recovery at the end of 1992 and the first half of 1993 to -5 ppb yr^{-1}, remaining relatively constant for the rest of the period. The recovery is not captured in the model, irrespective of the wetland emissions used. The explained growth rate in the model remains stable in the second half of 1993 and first half of 1994 and, in the case of ORCHIDEE emissions, decreases again in the second half of 1994.

3.2 Unexplained CH_4 variability

As explained in Section 2.2, CH_4 observations are used in a first step to quantify the mismatch between the model and observations. This nudging amount is analysed further to better understand the possible reasons for this mismatch.

The global deseasonalised nudging amounts for ‘Base1’ and ‘Base2’ are shown in Figure 5. Due to the difference of about 100 Tg yr^{-1} in the global emissions from the two wetland inventories, the global nudging amount also shows an offset of similar magnitude. The global nudging over the period 1990 to 1995 is close to 0 with ORCHIDEE, and about 100 Tg yr^{-1} with LPJ. However, there is quite some variability for both simulations within a range of about 50 Tg yr^{-1}. In the first period of the simulation, the nudging term for the ORCHIDEE simulations varies between 0 and -20 Tg yr^{-1}, and between 75 and 105 Tg yr^{-1} for LPJ. The nudging increases by 25-30 Tg yr^{-1} during the first half of 1993 for both the ‘Base1’ and ‘Base2’ because the increase in the observed CH_4 growth rate in this period is not reproduced by the explained growth rate. Between the second half of 1993 and the end of 1995, the nudging term for the two simulations shows similar variations, between 5 and 30 Tg yr^{-1} for ORCHIDEE, and between 100 and 125 Tg yr^{-1} for LPJ.

To better quantify the nudging term, the zonal mean nudging amounts for the two simulations as a function of time are given in Figure 6c and 6d. The zonal mean emission and sink strengths for the ‘Base1’ simulation are also shown for comparison in Figure 6a and 6b. In both simulations, nudging is predominantly needed in the Northern Hemisphere, where most CH_4 is emitted. This suggests that the uncertainties related to the CH_4 sources dominate the ones related to the sink or to transport, which occur in both hemispheres. Positive nudging is needed in the tropics in both hemispheres with a maximum during autumn, and following the position of the inter-tropical convergence zone (ITCZ). This suggests either missing emissions from tropical wetlands or biomass burning, or an overestimated strength of the tropical OH sink. In the northern mid-latitudes, the model overestimates CH_4 concentrations in the winter, and underestimates concentrations in the summer. This suggests a missing seasonality in one of the CH_4 budget terms. Positive nudging amounts at northern high-latitudes are needed throughout the two simulations, except for ‘Base1’ during autumn, where negative nudging is required. These might be related to underestimated anthropogenic emissions, as well as to errors in transport or vertical mixing, since both natural emissions and the CH_4 sink are almost negligible at high-latitudes during winter.

In Figure 6e and 6f the nudging for the year 1990 was subtracted from the whole time series, and a 12-month running mean was applied. These plots thus highlight the potential missing IAV in the model compared to observations. For both simulations we find a missing decrease in the CH_4 burden in the northern tropics during 1991 to 1993. This points to either a missing decrease in both wetland emission inventories in this region, or to potential uncertainties in tropical biomass burning. At northern mid-latitudes the CH_4 emissions are dominated by anthropogenic emissions, therefore the missing CH_4 increase revealed in this region suggests that the decrease in anthropogenic emissions over Europe, North America and the FSU in this time period might be overestimated. When using ORCHIDEE emissions we find an additional missing increase in the southern tropics from 1992 onwards, in particular in 1993 and 1995.

4 Discussion

We have quantified for the first time all known major drivers of CH_4 variability in the early 1990s in a global chemistry and transport model. Previous attempts to explain the CH_4 evolution in this period were the inverse modelling studies of W04 and B06. The sensitivity of the CH_4 growth rate to most of the drivers presented here was also investigated in our previous study Bândă et al. (2013), using a column chemistry model. Other bottom-up studies have focused on only one of the potential causes of CH_4 variability during the post-Pinatubo period. In the following sections we compare our results to previous top-down and bottom-up studies, and discuss potential sources of uncertainty in our results.

4.1 Comparison to inverse modelling studies

The CH_4 inverse modelling studies of W04 and B06 included the post-Pinatubo period. The OH fields used were derived by different methods. W04 used parameterised OH fields based on chemistry model results. Changes in meteorology, O_3 column, concentrations of CO and NMVOC were included in their parameterisation. However, stratospheric aerosols from the Pinatubo eruption were not included. The OH fields in B06 were determined from an inversion of methyl-chloroform observations, and might be affected by uncertainties in emissions of methyl chloroform.

With regard to the either applied or inferred OH sink variations, the inversion studies for this time period are only partly in line with our simulated variations in the OH sink, including the combined effect of stratospheric aerosols, stratospheric O_3 depletion and tropospheric emissions of CO and NMVOCs. We will now discuss the comparison between our results with these earlier studies for the different time periods: (i) the sharp decrease in the CH_4 growth rate in the second half of 1991 throughout 1992, (ii) the subsequent increase in the CH_4 growth rate in 1993, (iii) the moderate growth rates over the years 1994 and 1995, and (iv) the decrease in CH_4 growth rate over the period 1990 to 1995.

1991-1992

W04 inferred a slight decrease in the OH sink of CH_4 in 1991 compared to 1990, and an increase of about 10 $\mathrm{Tg\,yr^{-1}}$ in 1992. In B06, a decrease of about 25 $\mathrm{Tg\,yr^{-1}}$ in the OH sink was found during 1990 to 1992. In our study we find smaller OH variations than both studies, with a decrease in the OH sink of CH_4 of about 5 $\mathrm{Tg\,yr^{-1}}$ in 1992 compared to 1990 and 1991. This reduction in OH is due to sulfate aerosols and atmospheric cooling, compensated by the OH increase caused by ozone depletion (see Table 1, Figure 3).

Based on their assumed OH concentrations, W04 obtained a 20-25 Tg decrease in wetland emissions in 1992 compared to 1991 and 1990. To explain the decrease in the CH_4 growth rate in 1992, B06 found a 35-40 $\mathrm{Tg\,yr^{-1}}$ decrease in wetland emissions in the first half of 1992. To compensate for their simultaneous decrease in OH sink, they found 5-10 Tg lower biomass burning emissions in 1992 than 1991 and 1993, and a 20 Tg decrease in anthropogenic emissions, which is sustained for the rest of the 1990s. With ORCHIDEE we applied a 25 $\mathrm{Tg\,yr^{-1}}$ emission decrease in 1992. Our nudging suggests that this decrease could reach 29 $\mathrm{Tg\,yr^{-1}}$, which is similar in magnitude to the other studies.

1993

The observed CH_4 growth rate partially recovers during 1993 from the strong decrease in the year 1992. In our study we capture the decrease in CH_4 growth rate in 1993 rather than 1992 due to a 22 Tg increase in the OH sink of CH_4 because of reduced ozone columns, biomass burning emissions and a recovery of sulfate aerosols. A partial recovery in wetland emissions is found in both inventories. This recovery might be underestimated, since an increase in the nudging term is needed to explain the observed growth rate. Both W04 and B06 found increases in the CH_4 sink of about 10 $\mathrm{Tg\,yr^{-1}}$ during 1993. Similarly to our study, W06 simulate a continued decrease in CH_4 growth rate rather than a recovery. In B06, increases in wetland and biomass burning emissions in 1993 are found to overwhelm the increase in the CH_4 sink, leading to an increase in the CH_4 growth rate.

1994-1995

The OH sink of CH_4 showed variations of 3 to 5 $\mathrm{Tg\,yr^{-1}}$ in W06 in the years 1993 to 1995, while an increase of about 15 $\mathrm{Tg\,yr^{-1}}$ in the years 1993 to 1995 was obtained in B06. In agreement to B06, we find a 12 $\mathrm{Tg\,yr^{-1}}$ increase in the OH sink of CH_4 between 1993 and 1995 due to the recovery of the anomaly in temperature, water vapour and stratospheric aerosols caused by the eruption.

Similar to the study of W06, we find that the decrease in the CH_4 growth rate over the period 1990 to 1995 can be entirely explained by an increase in the OH sink of CH_4, rather than by changes in emissions. In B06, however, this decrease in CH_4 growth rate is explained by a decrease in anthropogenic emissions.

The more recent study of Pison et al. (2013) extended the study of B06 by using both methyl chloroform and CH_4 observations to constrain OH concentrations in their INVARR inversion. Smaller OH variability is found in this case compared to B06, and their derived global emission changes are more in line with W04 and with the emissions applied in our first simulation set.

The 1.6% IAV we find for the CH_4 loss by reaction with OH supports the conclusion of Montzka et al. (2011) that OH concentrations are buffered against atmospheric perturbations, having an IAV of about 2%. The large OH inter-annual variations, often exceeding 10%, previously found for the 1990s using methyl chloroform observations are not produced in our chemistry-transport simulations (Prinn et al., 2005; Bousquet et al., 2005).

4.2 Comparison to previous bottom-up studies

In (Bândă et al., 2013), we analysed the CH_4 growth rate variability after the Pinatubo eruption using a column chemistry model. The timing of the minimum CH_4 growth rate reported in that study is similar to the one found in this three-dimensional study, implying that the delay compared to observations is a result of uncertainties in model input rather than model setup. However, some differences between the two studies occur in the magnitude and contribution of the different processes to the CH_4 growth rate decrease in 1991 to 1993. In Bândă et al. (2013), the overall explained growth rate decrease was found to be 12 ppb yr^{-1}, while here we find only 8 to 10 ppb yr^{-1}. A 5 ppb yr^{-1} decrease was found due to CH_4, NO_X and CO anthropogenic emission changes. This is similar to the decrease of 6 ppb yr^{-1} due to changes in non-wetland emissions obtained in this study. However, our current estimate also includes variations of emissions from biomass burning, natural emissions of CO and NMVOC. The sulfate aerosol and O_3 column effects also differ by 2 to 3 ppb yr^{-1} from the estimates presented in Bândă et al. (2013), probably because the regional distribution of these effects could not be taken into account in the simplified column model approach. Furthermore, our previous study showed that CH_4 concentrations are affected for a long time period after a perturbation is applied due to the CH_4 lifetime of about 10 years. This delayed effect can be seen here for stratospheric sulfur, where a small negative difference in the CH_4 growth rate is found towards the end of the simulation period (Figure 3). The delayed effect that a perturbation in a driver of CH_4 variability has on the CH_4 growth rate also occurs in our other simulations. However, it is in general overwhelmed by the instantaneous effect of variability in the CH_4 driver.

Other studies have focused on only one of the drivers of CH_4 variability after the Pinatubo eruption. Bekki and Pyle (1994) found a decrease in CH_4 growth rate of 7 ppb yr^{-1} globally due to stratospheric O_3 using a two dimensional model between spring 1991 and autumn 1992. Here we obtain a comparable estimate of 5 ppb yr^{-1} decrease over the period 1991 to autumn 1993 due to the pronounced stratospheric O_3 depletion in the tropics and northern mid-latitudes in 1993.

Using a two-dimensional chemistry and transport model, Bekki and Law (1997) investigated the effect of temperature on both chemistry and wetland emissions in 1991-1992. They found that the temperature decrease after Pinatubo led to a 4 ppb yr^{-1} increase in the global CH_4 growth rate between mid-1991 and mid-1992, similar to our meteorological effect of 5 ppb yr^{-1}. By applying a $Q_{10} = 2$ temperature sensitivity of CH_4 emissions (Dunfield et al., 1993), they found that CH_4 emissions from wetlands would decrease the CH_4 growth rate by 2 ppb yr^{-1} in the same period. This is similar to our result using LPJ wetland emissions. The ORCHIDEE inventory gives a much larger decrease in the CH_4 growth rate of 9 ppb yr^{-1}, which overwhelms the meteorological effect on the CH_4 sink. This shows that the climate sensitivity of wetland emissions is larger in ORCHIDEE, where changes in wetland extent are taken into account.

Stratospheric aerosols were found to enhance the Brewer-Dobson circulation after the Pinatubo eruption (Aquila et al., 2013). This change in the dynamics of the atmosphere might also affect

CH_4 concentrations. Schauffler and Daniel (1994) hypothesized that increased exchange between the stratosphere and troposphere might be responsible for the decrease in CH_4 growth rate observed in 1992. By performing an additional simulation where only temperature and humidity were fixed to 1990 values, we found that the meteorological effect is dominated by the effect of these two variables (results not shown). The global impact of changes in ERA-Interim wind fields is marginal. The wind fields in ERA-Interim have some uncertainty for the first weeks after the eruption related to the fact that Pinatubo aerosols are not explicitly accounted for. However, the longer-term effect on temperature and the corresponding dynamical effect are included in ERA-Interim through the assimilation of satellite radiances.

Dlugokencky et al. (1994) and Law and Nisbet (1996) hypothesized that the emission decline in the FSU could have had a significant contribution to the decrease in CH_4 concentrations during 1992, because the decrease is primarily found in the Northern Hemisphere. However, our results indicate a missing CH_4 burden decrease in 1992 which originates in the northern tropics (Figure 6). Furthermore, a missing increase in CH_4 concentrations is found in the Northern Hemisphere extratropics, pointing to a potential missing source in this region rather than reduced emissions due to gas leak fixes. Furthermore, the overall decrease in growth rate between 1990 and 1996 is captured by our model, and can be attributed to stratospheric O_3 decrease over this period, and decreases in biomass burning and biogenic emissions of NMVOC and CO. We acknowledge, however, that the nudging procedure used here introduces some uncertainty in providing the location of missing emissions. The procedure attributes the source-sink mismatch at the dateline to sources or sinks in the same 10-degree latitude band. Potential sub-monthly transport of emissions from other latitudes is not taken into account. To further constrain the sources of model-measurement mismatch, an inverse modelling study should be performed to estimate the variability of the CH_4 sources using modelled OH variability.

4.3 Potential sources of uncertainty

In this study all known major drivers of CH_4 variability have been included. We estimate that potential missing processes had a minor effect on CH_4 concentrations, and would therefore not significantly affect our results. Such processes are the radiative effects of ash and water vapour injected in the stratosphere by the eruption, and the effect of sulfur deposition on CH_4 emissions from wetlands. Ash particles emitted by the eruption have a short lifetime of a few days (Guo et al., 2004; Niemeier et al., 2009), and were found to have a negligible effect on global radiation. Changes in water vapour are included through ERA-Interim reanalysis, and might contain some uncertainties (Dessler et al., 2014). Sulfur deposition has also been proposed to affect CH_4 emissions from wetlands (Gauci and Chapman, 2006). This effect is not included in our input data. In Bândă et al. (2013) we made a rough estimate of this effect, and found it to be of the order of 1 Tg CH_4 yr^{-1} for the Pinatubo eruption.

The zonal mean nudging term in our model points to either underestimated emissions or overestimated sinks in the tropics and during summer at mid-latitudes. An overestimated source is identified at mid-latitude during winter. Uncertainties in the OH sink of CH_4 might relate to uncertainties in the chemistry. CO concentrations in TM5 are underestimated at the northern mid-latitudes (Huijnen et al., 2010; van Noije et al., 2014), which might lead to overestimated OH concentrations in this region. An overestimate in OH concentrations at northern mid-latitudes and an overestimated north-south gradient in global chemistry models is also found from methyl chloroform observations in Patra et al. (2014). In the tropics, OH uncertainties might arise due to NMVOC chemistry, and are discussed in more detail below. Other uncertainties in tropical OH might relate to NO_X and CO emission factors from biomass burning. CO decreases OH concentrations, while NO_X increases OH recycling, therefore the overall effect of biomass burning emissions on OH are strongly dependent on the emission factors of these species, which are uncertain in tropical region in the early 1990s (Schultz et al., 2008).

Our results show that the decrease in CH_4 growth rate observed in 1992 is reasonably well explained by the processes considered here. However, the exact timing of the minimum growth rate is captured 6 to 9 months later than in the observations. Since missing processes are estimated to have a small impact on CH_4 variability in the early 1990s, the mismatch between modelled and measured CH_4 concentrations can only be related to uncertainties in either input data or modelled CH_4 processes. Measurement uncertainty might also contribute to the mismatch. The differences given by the two measurement-based estimates of the global CH_4 growth rate in Figure 4 show that uncertainties can be of the order of 2-3 $\text{ppb}\,\text{yr}^{-1}$. Our input data and chemical processes related to aerosols, O_3 and meteorological effects are fairly well studied and understood. The uncertainty related to these processes is in the order of 10-20%, and cannot explain the different timing of the decrease in CH_4 growth rate between the model and observations.

Larger uncertainties are related to the CH_4 emissions. The differences between the CH_4 emissions from the ORCHIDEE and LPJ inventories, both in terms of magnitude and IAV (Table 1), show that there are still many unknowns in the processes governing emissions from wetlands. One of the most important differences between the two models is the fact that ORCHIDEE simulates changes in wetland extent, while LPJ uses fixed wetland extent. This might be the cause for the larger IAV in ORCHIDEE, and for the higher climate sensitivity. Large differences in the response of ten wetland emission models to a temperature perturbation were also found in the WETCHIMP model intercomparison project, showing that a better understanding of wetland processes is needed (Melton et al., 2013).

Biomass burning emission uncertainties could also contribute to the mismatch between model and observations. However, given the IAV in biomass burning emissions in both the RETRO and the more recent GFED emission inventory of about 3 Tg $CH_4\,\text{yr}^{-1}$, it is unlikely that uncertainties in biomass burning CH_4 emissions could be the sole reason for the mismatch. As explained above, it is also unlikely that anthropogenic emission changes due to gas leak fixes within the FSU contributed to the mismatch.

We find a significant impact of CO and NMVOC emission changes on the CH_4 removal by OH. Some uncertainty is associated with NMVOC emission changes and their effect on CH_4 chemistry in the period after Pinatubo. Natural emissions of isoprene respond to both changes in climate and in solar radiation (Telford et al., 2010; Wilton et al., 2011). A decrease in surface temperatures would lead to a reduction in isoprene emissions. Concerning the effects of radiation, the increase in diffuse radiation after the eruption, leading to deeper penetration into canopies, has been shown to have overwhelmed the effect of decreased direct radiation in terms of plant growth (Mercado et al., 2009). Therefore the increase in diffuse radiation would have increased isoprene emissions. However, in this study only the effect of climate change and the effect of decrease in total shortwave radiation after the eruption are included through the MEGAN inventory. The isoprene emissions in MEGAN show a decline of 50 $\mathrm{Tg\,yr^{-1}}$ globally during 1992, likely due to the decrease in surface temperature and global shortwave radiation. The CH_4 growth rate decreases by about 4 $\mathrm{ppb\,yr^{-1}}$, or 11 $\mathrm{Tg\,yr^{-1}}$ due to changes in emissions of other species than CH_4 including isoprene. These changes are of similar magnitude as found in Telford et al. (2010), where a 40 Tg decrease in isoprene emissions between 1990 and 1992 resulted in a 5 Tg increase in CH_4 removal by OH. The estimated effect of NMVOC emissions on CH_4 concentrations has several sources of uncertainty. Firstly, including the effect of Pinatubo on diffuse radiation might have led to increased NMVOC emissions in 1991-1992, and an even stronger decrease in 1993, when the aerosols were removed from the atmosphere. Secondly, recent studies have shown that the sensitivity of OH concentrations to NMVOC is smaller than previously thought (Stone et al., 2011; Rohrer et al., 2014). The CBM4 chemistry scheme used here does not include an updated isoprene chemistry mechanism, and might exhibit a too high OH sensitivity to isoprene. Telford et al. (2010) used a chemistry scheme that includes the Mainz isoprene mechanism, a parameterisation based on the Master Chemical Mechanism (MCM), which was also shown to misrepresent OH recycling in VOC-rich environments (Pöschl et al., 2000; Stone et al., 2011). Nevertheless, it is important to take NMVOC emission changes into account for evaluating CH_4 variability. Due to the potentially overestimated OH sensitivity, our calculated effect on CH_4 can be seen as an upper estimate.

The latitudinal nudging term needed to correct the mismatch between modelled and observed CH_4 mixing ratios and presented in Sect 3.2 is calculated from measurements at five remote stations. Some uncertainty exists in these terms due to possible observational uncertainty and shortcomings of the nudging procedure. An indication of the observational uncertainty is given in Figure 4, where two observation-based estimates of the global mean CH_4 growth rate variations are shown. The GLOBALVIEW data uses a more complete set of stations, but might contain measurements affected by nearby emissions. Furthermore, additional processing is done to gap-fill and homogenise the station data. The two estimates are in good agreement except for the year 1991, where they differ by about 4 ppb/yr. Some uncertainty also exists in the timing and location of the missing emission variations given by the nudging term. Our nudging procedure is in general able to capture the global growth rate variations. However, because the nudging corrects the amount of CH_4 in the zonal band where the mismatch occurs, this procedure does not account for sub-monthly transport between zonal bands. An inverse modelling setup would be needed to exploit all available measurements to better resolve the sources of mismatch.

5 Conclusions

The processes responsible for CH_4 variability in the early 1990s have been investigated in the global chemistry and transport model TM5. Known drivers of CH_4 variations include: (i) photochemical effects of stratospheric sulfur from Pinatubo and (ii) of stratospheric O_3 changes, (iii) temperature and humidity perturbations, and their effect on CH_4 chemistry, (iv) variations in CH_4 emissions from wetlands, (v) biomass burning and (vi) anthropogenic sources, and (vii) changes in emissions of other compounds and their effect on OH. We find that all these processes contributed in a significant way to the CH_4 growth rate variations in the early 1990s.

The 'explained' growth rate evolution falls within the observational range during 1991. However, the increase in growth rate modelled at the end of 1991 using wetlands CH_4 emissions from LPJ is not found in the observations. The observed decrease of about 10 $\mathrm{ppb\,yr^{-1}}$ in CH_4 growth rate during the year 1992 is captured by the model with a delay of half a year to one year. We have used two inventories for CH_4 emission from wetlands to explore the potential role of uncertainties in this emission sector. Although they have a significantly different variability, the two inventories give a similar performance in capturing the global CH_4 variations. When using ORCHIDEE, the global CH_4 growth rate is better captured in 1990 to 1993, while using LPJ we are able to reproduce better the CH_4 growth rate at the end of the analysed period. The increase in CH_4 in 1993 is not captured by either of the two scenarios. According to our breakdown in individual causes for CH_4 growth rate changes, the overall decrease in the CH_4 growth rate of 5 $\mathrm{ppb\,yr^{-1}}$ during 1990 to 1995 is explained by the observed decrease in O_3 column due to the 11-year cycle in solar activity, and by the estimated decrease in CO and NMVOC emissions in this period.

By analysing the nudging term, we find that the mismatch most likely originates in the northern tropical region. Since the effects of UV changes and temperature changes on OH are considered to be robust, the most likely source of missing variability is natural CH_4 emissions from wetlands. Uncertainties in tropical biomass burning emissions, and in biogenic NMVOC emissions and their effect on OH might have also contributed to the mismatch between the modelled and observed CH_4 concentrations. Modelling CH_4 emissions from wetlands is a challenging topic, due to the large spatial and temporal variability of these ecosystems. The large differences between the two emission datasets used here in terms of CH_4 emission amount and variability show that further research is needed to understand the factors driving emissions from wetlands and their response to environmental factors. Furthermore, the effect of changes in diffuse radiation and sulfur deposition after the eruption are not taken into account in the inventories used in this study. Another source of uncertainty are changes in NMVOC emissions, as well as the impact of NMVOC changes on OH. Further study is recommended using an updated isoprene chemistry scheme that considers the OH recycling by NMVOC, and using NMVOC emission models that take into account the effect of both direct and diffuse radiation. Finally, some uncertainty exists in our nudging procedure. An inverse modelling approach using OH fields from this study and all available CH_4 station measurement data could better resolve the sources and timing of model-measurement mismatch. This might, almost 25 years after the Pinatubo eruption, further improve our knowledge on the drivers of CH_4 growth rate variations.

Appendix A: Validation of the two-step nudging setup

We use a two-step method to simulate realistic CH_4 concentrations. In a first step, 'Base1' and 'Base2' scenarios are run with near-surface CH_4 mixing ratios nudged towards the zonal mean background mixing ratios inferred from measurements at the five stations of South Pole, Cape Grim, Mauna Loa, Niwot Ridge, Barrow, and Alert. The nudging amount is stored on a monthly basis for each 10-degree latitude band, and used in the second step. In this second step, CH_4 is no longer constrained by observations, but instead the nudging amount calculated in the first step is applied as an emission in all scenarios in the lower 2 km.

Figure 7 presents the global and dateline monthly mean CH_4 concentrations and the deseasonalised growth rates obtained in the two runs of 'Base1', and their comparison with 'Background5' observations. Please note that we show here absolute CH_4 growth rates, and not variations with respect to 1990 as shown in Figure 4. Also note that the actual CH_4 growth rates in 'Base1' are plotted, unlike in Figures 3 and 4 and where differences between simulations were presented. CH_4 concentrations at the dateline were nudged in the first step to the concentration values indicated by 'Background5'. Therefore, the fact that the CH_4 dateline mean concentrations follow reasonably well the observations is a result of the nudging procedure. The global surface mean concentrations in the model show similar variations as the dateline mean, but with concentrations of 10 to 15 ppb higher. This is due to the fact that the dateline crosses the Pacific Ocean, and is remote from CH_4 sources, while in the global mean both remote and polluted areas are included. The observed deseasonalised CH_4 growth rate is well reproduced in the model both by the dateline mean and by the surface mean. The modelled dateline growth rate is within 1 ppb/yr from the observed one, while the model global mean is within 2 ppb/yr. Both the surface mean and the dateline mean of the two steps from the model follow well the observed growth rate variations, with a slightly better performance of the dateline towards the end of the simulation.

The global mean and dateline mean concentrations and growth rates of the second step are nearly identical to those of the first step. This shows that the procedure in which the correction is applied does not significantly influence the results, and that the simulation results of the two steps give a similar performance in capturing the observed CH_4 growth rates.

Appendix B: Additivity between drivers of CH_4 variability

In Figure 3 we have shown the combined effect of the drivers for CH_4 variability assuming additivity between the different drivers. We verify this assumption by using results from the 'FixAll1' simulation, where all drivers of CH_4 were fixed to 1990 values. Figure 8 shows the combined effect of the 7 drivers for CH_4 variability found from the sum of individual drivers for the first simulation set (also shown in figure 5.4 and labeled 'All Orchidee'), and the combined effect found from the difference between 'Base1' and 'FixAll1'. The two global CH_4 growth rate curves nearly overlap each other, with differences less than 0.2 ppb/yr. This shows that indeed the assumption of additivity is valid.

Acknowledgements. We thank Bruno Ringeval and Joe Melton for providing the ORCHIDEE emission data. This work was supported by the Netherlands Organisation for Scientific Research (NWO). We thank the SURF Foundation (www.surfsara.nl) for their support in using the Dutch national e-infrastructure.

References

Aan de Brugh, J. M. J., Schaap, M., Vignati, E., Dentener, F., Kahnert, M., Sofiev, M., Huijnen, V., and Krol, M. C.: The European aerosol budget in 2006, Atmospheric Chemistry and Physics, 11, 1117–1139, doi:10.5194/acp-11-1117-2011, 2011.

Andres, R. J. and Kasgnoc, A. D.: A time-averaged inventory of subaerial volcanic, Journal of Geophysical Research, 103, 25,251–25,261, doi:10.1029/98JD02091, 1998.

Aquila, V., Oman, L. D., Stolarski, R., Douglass, A. R., and Newman, P. A.: The Response of Ozone and Nitrogen Dioxide to the Eruption of Mt. Pinatubo at Southern and Northern Midlatitudes, Journal of the Atmospheric Sciences, 70, 894–900, doi:10.1175/JAS-D-12-0143.1, 2013.

Bândă, N., Krol, M., van Weele, M., van Noije, T., and Röckmann, T.: Analysis of global methane changes after the 1991 Pinatubo volcanic eruption, Atmos. Chem. Phys., 13, 2267–2281, doi:10.5194/acp-13-2267-2013, http://www.atmos-chem-phys.net/13/2267/2013/http://www.atmos-chem-phys.net/13/2267/2013/acp-13-2267-2013.pdf, 2013.

Bândă, N., Krol, M., van Noije, T., van Weele, M., Williams, J. E., Le Sager, P., Niemeier, U., Thomason, L., and Röckmann, T.: The effect of stratospheric sulfur from Mount Pinatubo on tropospheric oxidizing capacity and methane, Journal of Geophysical Research: Atmospheres, p. 2014JD022137, doi:10.1002/2014JD022137, 2014.

Bekki, S. and Law, K. S.: Sensitivity of the atmospheric CH4 growth rate to global temperature changes observed from 1980 to 1992, Tellus, 49B, 409–416, 1997.

Bekki, S. and Pyle, J. A.: A two-dimensional modeling study of the volcanic eruption of Mount Pinatubo, Journal of Geophysical Research, 99, 18,861 – 18,869, 1994.

Bekki, S., Law, K. S., and Pyle, J. A.: Effect of ozone depletion on atmospheric CH4 and CO concentrations, Nature, 371, 595–597, 1994.

Bousquet, P., Hauglustaine, D. A., Peylin, P., Carouge, C., and Ciais, P.: Two decades of OH variability as inferred by an inversion of atmospheric transport and chemistry of methyl chloroform, Atmospheric Chemistry and Physics, 5, 2635–2656, 2005.

Bousquet, P., Ciais, P., Miller, J. B., Dlugokencky, E. J., Hauglustaine, D. A., Prigent, C., Van der Werf, G. R., Peylin, P., Brunke, E.-G., Carouge, C., Langenfelds, R. L., Lathière, J., Papa, F., Ramonet, M., Schmidt, M., Steele, L. P., Tyler, S. C., and White, J.: Contribution of anthropogenic and natural sources to atmospheric methane variability., Nature, 443, 439–43, doi:10.1038/nature05132, 2006.

Dalsøren, S. B. and Isaksen, I. S. A.: CTM study of changes in tropospheric hydroxyl distribution 1990–2001 and its impact on methane, Geophysical Research Letters, 33, L23 811, doi:10.1029/2006GL027295, 2006.

Dee, D. P., Uppala, S. M., Simmons, A. J., Berrisford, P., Poli, P., Kobayashi, S., Andrae, U., Balmaseda, M. A., Balsamo, G., Bauer, P., Bechtold, P., Beljaars, A. C. M., Berg, L. V. D., Bidlot, J., Bormann, N., Delsol, C., Dragani, R., Fuentes, M., Geer, A. J., Haimberger, L., Healy, S. B., Hersbach, H., Holm, E. V., Isaksen, L., and Kallberg, P.: The ERA-Interim reanalysis : configuration and performance of the data assimilation system, Quarterly Journal of the Royal Meteorological Society, 137, 553–597, doi:10.1002/qj.828, 2011.

Denman, K., Brasseur, G., Chidthaisong, A., Ciais, P., Cox, P., Dickinson, R., Hauglustaine, D., Heinze, C., Holland, E., Jacob, D., Lohmann, U., Ramachandran, S., Dias, P. d. S., Wofsy, S., and Zhang, X.: Couplings Between Changes in the Climate System and Biogeochemistry. In: Climate Change 2007: The Physical

Science Basis. Contribution of Working Group I to the Fourth Assessment Report of the Intergovernmental Panel on Climate Change [Solomon, S., D. Qin, Tech. rep., Cambridge University Press, Cambridge, United Kingdom and New York, NY, USA, 2007.

Dentener, F., Peters, W., Krol, M., Weele, M. V., and Bergamaschi, P.: Interannual variability and trend of CH 4 lifetime as a measure for OH changes in the 1979 – 1993 time period, Time, 108, doi:10.1029/2002JD002916, 2003.

Dessler, A. E., Schoeberl, M. R., Wang, T., Davis, S. M., Rosenlof, K. H., and Vernier, J.-P.: Journal of Geophysical Research : Atmospheres, Journal of Geophysical Research: Atmospheres, 119, 12,588–12,598, doi:10.1002/2014JD021712.Received, 2014.

Dlugokencky, E. J., Masaire, K. A., Lang, P. M., Tans, P. P., Steele, L. P., and Nisbet, E. G.: A dramatic decrease in the growth rate of atmospheric methane in the northern hemisphere during 1992, Geophysical Research Letters, 21, 45–48, 1994.

Dlugokencky, E. J., Dutton, E. G., Novelli, P. C., Tans, P. P., Masarie, K. A., Lantz, K. O., and Madronich, S.: Changes in CH4 and CO growth rates after the eruption of Mt. Pinatubo and their link with changes in tropical tropospheric UV flux, Geophysical Research Letters, 23, 2761–2764, 1996.

Dunfield, P., Knowles, R., Dumont, R., and Moore, T. R.: Methane production and consumption in temperate and subarctic peat soils: Response to temperature and pH, Soil Biology and Biochemistry, 25, 321–326, http://www.sciencedirect.com/science/article/pii/0038071793901304, 1993.

Gauci, V. and Chapman, S. J.: Simultaneous inhibition of CH4 efflux and stimulation of sulphate reduction in peat subject to simulated acid rain, Soil Biology and Biochemistry, 38, 3506–3510, doi:10.1016/j.soilbio.2006.05.011, http://linkinghub.elsevier.com/retrieve/pii/S0038071706002562, 2006.

Gauci, V., Blake, S., Stevenson, D. S., and Highwood, E. J.: Halving of the northern wetland CH 4 source by a large Icelandic volcanic eruption, Journal of Geophysical Research, 113, 1–8, doi:10.1029/2007JG000499, 2008.

GLOBALVIEW-CH4: Cooperative Atmospheric Data Integration Project - Methane. CD-ROM, NOAA ESRL, Boulder, Colorado [Also available on Internet via anonymous FTP to ftp://ftp.cmdl.noaa.gov, Path: ccg/ch4/GLOBALVIEW], 2009.

Grooß J.-U. and Russell III, J.: Technical note: A stratospheric climatology for O3, H2O, CH4, NOx, HCl and HF derived from HALOE measurements, Atmospheric Chemistry and Physics, 5, 2797–2807, 2005.

Guo, S., Bluth, G. J. S., Rose, W. I., Watson, I. M., and Prata, A. J.: Re-evaluation of SO2 release of the 15 June 1991 Pinatubo eruption using ultraviolet and infrared satellite sensors, Geochemistry Geophysics Geosystems, 5, doi:10.1029/2003GC000654, 2004.

Houweling, S., Dentener, F., and Lelieveld, J.: The impact of nonmethane hydrocarbon compounds on tropospheric photochemistry radical, Journal of Geophysical Research, 103, 10,673–10,696, 1998.

Huijnen, V., Williams, J., van Weele, M., van Noije, T., Krol, M., Dentener, F., Segers, A., Houweling, S., Peters, W., de Laat, J., Boersma, F., Bergamaschi, P., van Velthoven, P., Le Sager, P., Eskes, H., Alkemade, F., Scheele, R., Nédélec, P., and Pätz, H.-W.: The global chemistry transport model TM5: description and evaluation of the tropospheric chemistry version 3.0, Geoscientific Model Development, 3, 445–473, doi:10.5194/gmd-3-445-2010, 2010.

Huijnen, V., Williams, J. E., and Flemming, J.: Modeling global impacts of heterogeneous loss of HO2 on cloud droplets, ice particles and aerosols, Atmospheric Chemistry and Physics Discussions, 14, 8575–8632, doi:10.5194/acpd-14-8575-2014, 2014.

Kirschke, S., Bousquet, P., Ciais, P., Saunois, M., Canadell, J. G., Dlugokencky, E. J., Bergamaschi, P., Bergmann, D., Blake, D. R., Bruhwiler, L., Cameron-Smith, P., Castaldi, S., Chevallier, F., Feng, L., Fraser, A., Heimann, M., Hodson, E. L., Houweling, S., Josse, B., Fraser, P. J., Krummel, P. B., Lamarque, J.-F., Langenfelds, R. L., Le Quéré, C., Naik, V., O'Doherty, S., Palmer, P. I., Pison, I., Plummer, D., Poulter, B., Prinn, R. G., Rigby, M., Ringeval, B., Santini, M., Schmidt, M., Shindell, D. T., Simpson, I. J., Spahni, R., Steele, L. P., Strode, S. a., Sudo, K., Szopa, S., van der Werf, G. R., Voulgarakis, A., van Weele, M., Weiss, R. F., Williams, J. E., and Zeng, G.: Three decades of global methane sources and sinks, Nature Geoscience, 6, 813–823, doi:10.1038/ngeo1955, http://www.nature.com/doifinder/10.1038/ngeo1955, 2013.

Lamarque, J.-F., Bond, T. C., Eyring, V., Granier, C., Heil, a., Klimont, Z., Lee, D., Liousse, C., Mieville, a., Owen, B., Schultz, M. G., Shindell, D., Smith, S. J., Stehfest, E., Van Aardenne, J., Cooper, O. R., Kainuma, M., Mahowald, N., McConnell, J. R., Naik, V., Riahi, K., and van Vuuren, D. P.: Historical (1850–2000) gridded anthropogenic and biomass burning emissions of reactive gases and aerosols: methodology and application, Atmospheric Chemistry and Physics, 10, 7017–7039, doi:10.5194/acp-10-7017-2010, http://www.atmos-chem-phys.net/10/7017/2010/, 2010.

Law, K. S. and Nisbet, E. G.: Sensitivity of the CH4 growth rate to changes in CH4 emissions from natural gas and coal, Journal of Geophysical Research, 101, 14,387–14,397, 1996.

Lawrence, M. G., Joeckel, P., and von Kuhlmann, R.: What does the global mean OH concentration tell us?, Atmospheric Chemistry and Physics, 1, 37–49, 2001.

Lelieveld, J., Peters, W., Dentener, F. J., and Krol, M. C.: Stability of tropospheric hydroxyl chemistry, Journal of Geophysical Research, 107, D23, 4715, doi:10.1029/2002JD002272, 2002.

McCormick, M. P., Thomason, L. W., and Trepte, C. R.: Atmospheric effects of the Mt. Pinatubo eruption, Nature, 373, 399–404, 1995.

Melton, J. R., Wania, R., Hodson, E. L., Poulter, B., Ringeval, B., Spahni, R., Bohn, T., Avis, C. a., Beerling, D. J., Chen, G., Eliseev, a. V., Denisov, S. N., Hopcroft, P. O., Lettenmaier, D. P., Riley, W. J., Singarayer, J. S., Subin, Z. M., Tian, H., Zürcher, S., Brovkin, V., van Bodegom, P. M., Kleinen, T., Yu, Z. C., and Kaplan, J. O.: Present state of global wetland extent and wetland methane modelling: conclusions from a model intercomparison project (WETCHIMP), Biogeosciences, 10, 753–788, doi:10.5194/bg-10-753-2013, 2013.

Mercado, L. M., Bellouin, N., Sitch, S., Boucher, O., Huntingford, C., Wild, M., and Cox, P. M.: Impact of changes in diffuse radiation on the global land carbon sink, Nature, 458, 1014–1018, doi:10.1038/nature07949, 2009.

Metzger, S., Dentener, F., Pandis, S., and Lelieveld, J.: Gas/aerosol partitioning: 1. A computationally efficient model, Journal of Geophysical Research: Atmospheres, 107, ACH 16–1–ACH 16–24, doi:10.1029/2001JD001102, http://dx.doi.org/10.1029/2001JD001102, 2002.

Montzka, S. A., Dlugokencky, E. J., and Butler, J. H.: Non-CO2 greenhouse gases and climate change, Nature, 476, 43–50, doi:10.1038/nature10322, 2011.

Niemeier, U., Timmreck, C., Graf, H.-F., Kinne, S., Rast, S., and Self, S.: Initial fate of fine ash and sulfur from large volcanic eruptions, Atmospheric Chemistry and Physics, 9, 9043–9057, 2009.

Patra, P. K., Krol, M. C., Montzka, S. A., Arnold, T., Atlas, E. L., Lintner, B. R., Stephens, B. B., Xiang, B., Elkins, J. W., Fraser, P. J., Ghosh, A., Hintsa, E. J., Hurst, D. F., Ishijima, K., Krummel, P. B., Miller, B. R., Miyazaki, K., Moore, F. L., O'Doherty, S., Prinn, R. G., Steele, L. P., Takigawa, M., Wang, H. J., Weiss, R. F., Wofsy, S. C., and Young, D.: Observational evidence for interhemispheric hydroxyl-radical parity, Nature, 513, 219–223, doi:10.1038/nature13721, 2014.

Pison, I., Ringeval, B., Bousquet, P., Prigent, C., and Papa, F.: Stable atmospheric methane in the 2000s: key-role of emissions from natural wetlands, Atmospheric Chemistry and Physics, 13, 11 609–11 623, doi:10.5194/acp-13-11609-2013, 2013.

Pöschl, U., von Kuhlmann, R., Poisson, N., and Crutzen, P.: Development and Intercomparison of Condensed Isoprene Oxidation Mechanisms for Global Atmospheric Modeling, Journal of Atmospheric Chemistry, 37, 29–52, doi:10.1023/A:1006391009798, 2000.

Prinn, R. G., Huang, J., Weiss, R. F., Cunnold, D. M., Fraser, P. J., Simmonds, P. G., McCulloch, A., Harth, C., Reimann, S., Salameh, P., O'Doherty, S., Wang, R. H. J., Porter, L. W., Miller, B. R., and Krummel, P. B.: Evidence for variability of atmospheric hydroxyl radicals over the past quarter century, Geophysical Research Letters, 32, L07 809, doi:10.1029/2004GL022228, 2005.

Ringeval, B., de Noblet-Ducoudré, N., Ciais, P., Bousquet, P., Prigent, C., Papa, F., and Rossow, W. B.: An attempt to quantify the impact of changes in wetland extent on methane emissions on the seasonal and interannual time scales, Global Biogeochemical Cycles, 24, GB2003, doi:10.1029/2008GB003354, 2010.

Rohrer, F., Lu, K., Hofzumahaus, A., Bohn, B., Brauers, T., Chang, C.-C., Fuchs, H., Haseler, R., Holland, F., Hu, M., Kita, K., Kondo, Y., Li, X., Lou, S., Oebel, A., Shao, M., Zeng, L., Zhu, T., Zhang, Y., and Wahner, A.: Maximum efficiency in the hydroxyl-radical-based self-cleansing of the troposphere, Nature Geosci, 7, 559–563, 2014.

Schauffler, S. M. and Daniel, J. S.: On the effects of stratospheric circulation changes on trace gas trends, Journal of Geophysical Research, 99, 25,747–25,754, 1994.

Schultz, M. G., Heil, A., Hoelzemann, J. J., Spessa, A., Thonicke, K., Goldammer, J. G., Held, A. C., Pereira, J. M. C., and van het Bolscher, M.: Global wildland fire emissions from 1960 to 2000, Global Biogeochemical Cycles, 22, GB2002, doi:10.1029/2007GB003031, 2008.

Shepherd, T. G., Plummer, D. A., Scinocca, J. F., Hegglin, M. I., Fioletov, V. E., Reader, M. C., Remsberg, E., von Clarmann, T., and Wang, H. J.: Reconciliation of halogen-induced ozone loss with the total-column ozone record, Nature Geosci, 7, 443–449, doi:10.1038/ngeo2155, 2014.

Sindelarova, K., Granier, C., Bouarar, I., Guenther, A., Tilmes, S., Stavrakou, T., Müller, J.-F., Kuhn, U., Stefani, P., and Knorr, W.: Global dataset of biogenic VOC emissions calculated by the MEGAN model over the last 30 years, Atmos. Chem. Phys. Discuss., 14, 10 725–10 788, doi:10.5194/acpd-14-10725-2014, 2014.

Soden, B. J., Wetherald, R. T., Stenchikov, G. L., and Robock, A.: Global Cooling After the Eruption of Mount Pinatubo: A Test of Climate Feedback by Water Vapor, Science, 296, doi:10.1126/science.296.5568.727, 2002.

Spahni, R., Wania, R., Neef, L., van Weele, M., Pison, I., Bousquet, P., Frankenberg, C., Foster, P. N., Joos, F., Prentice, I. C., and van Velthoven, P.: Constraining global methane emissions and uptake by ecosystems, Biogeosciences, 8, 1643–1665, doi:10.5194/bg-8-1643-2011, 2011.

Stone, D., Evans, M. J., Edwards, P. M., Commane, R., Ingham, T., Rickard, a. R., Brookes, D. M., Hopkins, J., Leigh, R. J., Lewis, a. C., Monks, P. S., Oram, D., Reeves, C. E., Stewart, D., and Heard, D. E.: Isoprene oxidation mechanisms: measurements and modelling of OH and HO2 over a South-East Asian tropical rainforest during the OP3 field campaign, Atmospheric Chemistry and Physics, 11, 6749–6771, doi:10.5194/acp-11-6749-2011, 2011.

Telford, P., Braesicke, P., Morgenstern, O., and Pyle, J.: Reassessment of causes of ozone column variability following the eruption of Mount Pinatubo using a nudged CCM, Atmospheric Chemistry and Physics Discussions, 9, 5423–5446, doi:10.5194/acpd-9-5423-2009, http://www.atmos-chem-phys-discuss.net/9/5423/2009/, 2009.

Telford, P. J., Lathiere, J., Abraham, N. L., Archibald, A. T., Braesicke, P., Johnson, C. E., Morgenstern, O., O'Connor, F. M., Pike, R. C., Wild, O., Young, P. J., Hewitt, C. N., and Pyle, J.: Effects of climate-induced changes in isoprene emissions after the eruption of Mount Pinatubo, Atmospheric Chemistry and Physics, pp. 7117–7125, doi:10.5194/acp-10-7117-2010, 2010.

Tiedtke, M.: A comprehensive mass flux scheme for cumulus parameterization in large-scale models, Mon. Weather Rev., 117, 1779–1800, 1989.

van der A, R. J., Allaart, M. a. F., and Eskes, H. J.: Multi sensor reanalysis of total ozone, Atmospheric Chemistry and Physics, 10, 11 277–11 294, doi:10.5194/acp-10-11277-2010, http://www.atmos-chem-phys.net/10/11277/2010/, 2010.

van Noije, T. P. C., Sager, P. L., Segers, A. J., van Velthoven, P. F. J., Krol, M. C., Hazeleger, W., Williams, A. G., and Chambers, S. D.: Simulation of tropospheric chemistry and aerosols with the climate model EC-Earth, Geoscientific Model Development, 7, 2435–2475, doi:10.5194/gmd-7-2435-2014, 2014.

Vignati, E., Wilson, J., and Stier, P.: M7: An efficient size-resolved aerosol microphysics module for large-scale aerosol transport models, Journal of Geophysical Research: Atmospheres, 109, n/a–n/a, doi:10.1029/2003JD004485, http://dx.doi.org/10.1029/2003JD004485, 2004.

Vignati, E., Facchini, M., Rinaldi, M., Scannell, C., Ceburnis, D., Sciare, J., Kanakidou, M., Myriokefalitakis, S., Dentener, F., and O'Dowd, C.: Global scale emission and distribution of sea-spray aerosol: Sea-salt and organic enrichment, Atmospheric Environment, 44, 670–677, doi:10.1016/j.atmosenv.2009.11.013, http://linkinghub.elsevier.com/retrieve/pii/S1352231009009571, 2010.

Wang, J. S., Logan, J. A., Mcelroy, M. B., Duncan, B. N., Megretskaia, I. A., and Yantosca, R. M.: A 3-D model analysis of the slowdown and interannual variability in the methane growth rate from 1988 to 1997, Global Biogeochemical Cycles, 18, GB3011, doi:10.1029/2003GB002180, 2004.

Wania, R., Melton, J. R., Hodson, E. L., Poulter, B., Ringeval, B., Spahni, R., Bohn, T., Avis, C. a., Chen, G., Eliseev, a. V., Hopcroft, P. O., Riley, W. J., Subin, Z. M., Tian, H., van Bodegom, P. M., Kleinen, T., Yu, Z. C., Singarayer, J. S., Zürcher, S., Lettenmaier, D. P., Beerling, D. J., Denisov, S. N., Prigent, C., Papa, F., and Kaplan, J. O.: Present state of global wetland extent and wetland methane modelling: methodology of a model inter-comparison project (WETCHIMP), Geoscientific Model Development, 6, 617–641, doi:10.5194/gmd-6-617-2013, 2013.

Williams, J. E., Landgraf, J., Bregman, A., and Walter, H. H.: A modified band approach for the accurate calculation of online photolysis rates in stratospheric-tropospheric Chemical Transport Models, Atmospheric Chemistry and Physics, 6, 4137–4161, 2006.

Williams, J. E., Strunk, A., Huijnen, V., and van Weele, M.: The application of the Modified Band Approach for the calculation of on-line photodissociation rate constants in TM5: implications for oxidative capacity, Geoscientific Model Development, 5, 15–35, doi:10.5194/gmd-5-15-2012, 2012.

Wilton, D. J., Hewitt, C. N., and Beerling, D. J.: Simulated effects of changes in direct and diffuse radiation on canopy scale isoprene emissions from vegetation following volcanic eruptions, Atmospheric Chemistry and Physics, 11, 11 723–11 731, doi:10.5194/acp-11-11723-2011, 2011.

Table 1. Annual mean CH_4 sources and sinks, and their interannual variability (IAV). All values are in Tg yr^{-1}.

Category	Inventory or simulation	1990	1991	1992	1993	1994	1995	Mean	IAV
Natural wetlands	ORCHIDEE	273.9	276.6	251.7	262.1	272.1	260.8	266.2	11.9
	LPJ	167.4	163.9	161.9	165.6	167.7	169.3	166.1	2.6
Natural other	HYMN	43.0	43.0	43.0	43.0	43.0	43.0	43.0	-
Anthropogenic	EDGAR	256.7	256.2	257.2	256.4	257.3	260.0	257.3	1.2
Biomass burning	RETRO	19.5	21.2	23.0	17.8	20.4	16.5	19.7	3.0
Trop CH_4+OH	Base1	489.8	489.4	483.7	505.4	512.0	517.8	499.7	8.1
	Base2	487.9	487.5	482.8	504.6	511.2	517.1	498.5	7.9
Stratospheric sink	Base1	35.1	39.2	39.8	40.3	42.0	41.6	39.7	1.5
	Base2	33.	37.2	38.8	39.4	41.3	40.8	38.4	1.8
Soil sink	Base1	29.2	30.4	26.3	28.5	26.4	25.5	27.7	2.1
	Base2	27.1	26.8	27.0	27.2	26.9	27.5	27.1	0.3
Nudging	Base1	-11.3	-15.1	-18.9	3.5	23.1	11.9	-1.1	12.4
	Base2	88.8	89.3	68.2	98.5	120.0	100.1	94.1	18.7

Table 2. Setup of the simulations, including CH_4 wetland inventory used and drivers of CH_4 included in each simulation. The crosses indicate that the variability of a certain driver is included in the simulation. Otherwise the driver is not included (in the case of Pinatubo SO_2 and aerosol) or 1990 values are used throughout the simulation.

		Drivers of CH_4 variability included						
Simulation name	Inventory for CH_4 emissions from wetlands	Pinatubo SO_2 and aerosol	Stratospheric O_3	Meteorology	CH_4 wetland emissions	Natural emissions of CO, NMVOC and NH_3	Anthropogenic emissions of CH_4 and other compounds	Biomass burning emissions of CH_4 and other compounds
Set I								
Base1	ORCHIDEE	X	X	X	X	X	X	X
NoPinS1	ORCHIDEE		X	X	X	X	X	X
FixOzone1	ORCHIDEE			X	X	X	X	X
FixMet1	ORCHIDEE		X		X	X	X	X
FixWetl1	ORCHIDEE		X	X		X	X	X
FixEmis1	ORCHIDEE		X	X	X			
FixAll1	ORCHIDEE							
Set II								
Base2	LPJ	X	X	X	X	X	X	X
NoPinS2	LPJ		X	X	X	X	X	X
FixWetl2	LPJ		X	X	X		X	X

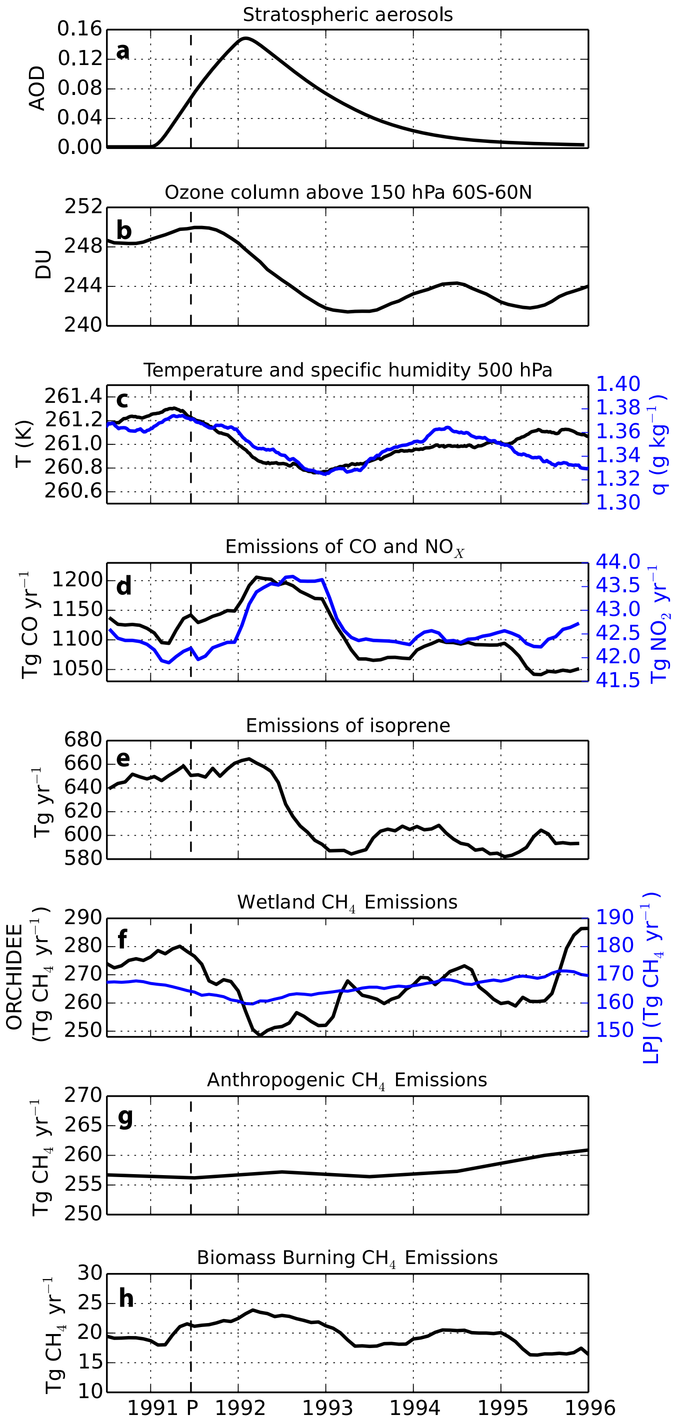

Figure 1. The drivers of CH_4 IAV in the early 1990s considered in this study. The black dashed line denotes the timing of the Pinatubo eruption.

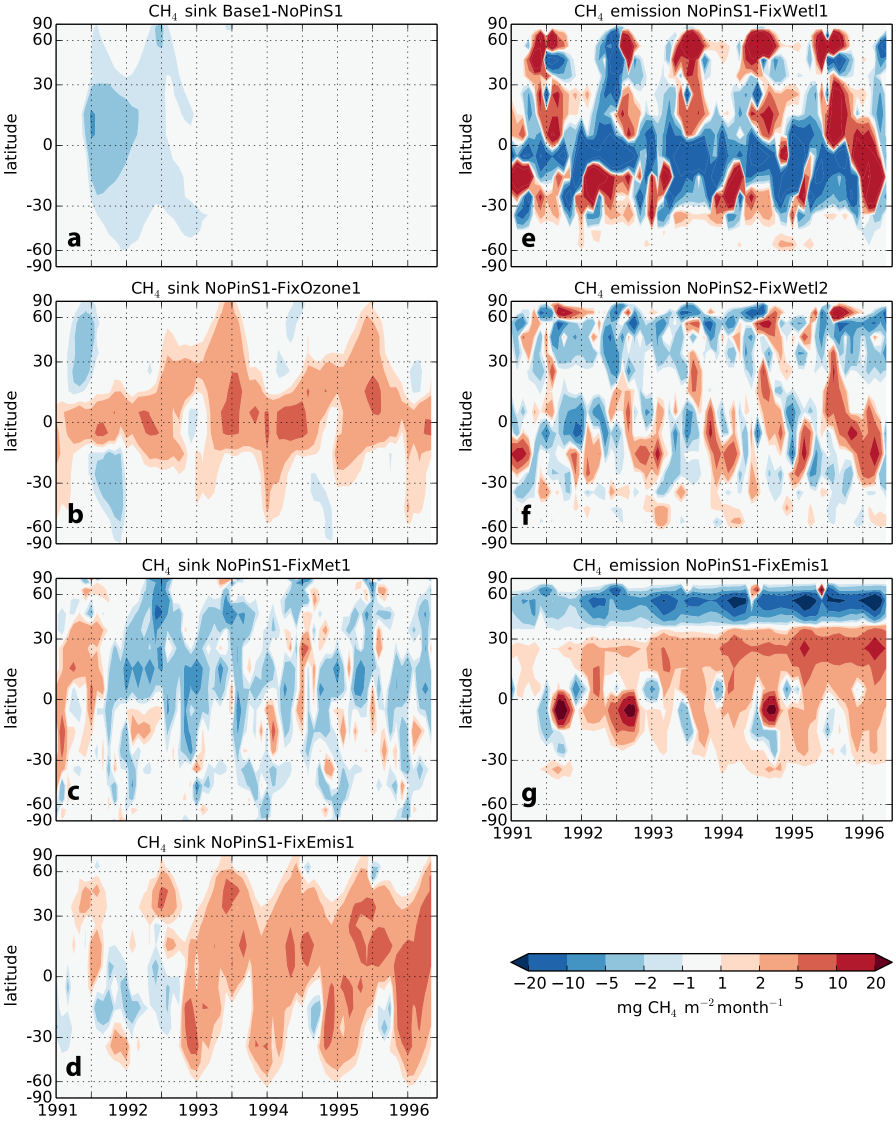

Figure 2. Zonal mean differences in the CH_4 budget terms caused by the different drivers of CH_4 variability, vertically integrated over the troposphere. Changes in the CH_4 sink by the reaction with OH are shown for the effects of a) stratospheric sulfur, b) stratospheric ozone, c) meteorology and d) emissions of CO, NO_X and NMVOC. CH_4 emission changes are shown for wetlands from e) ORCHIDEE and f) LPJ, g) for biomass burning and anthropogenic sectors. The years on the x-axis in this and later figures refer to the start of the year.

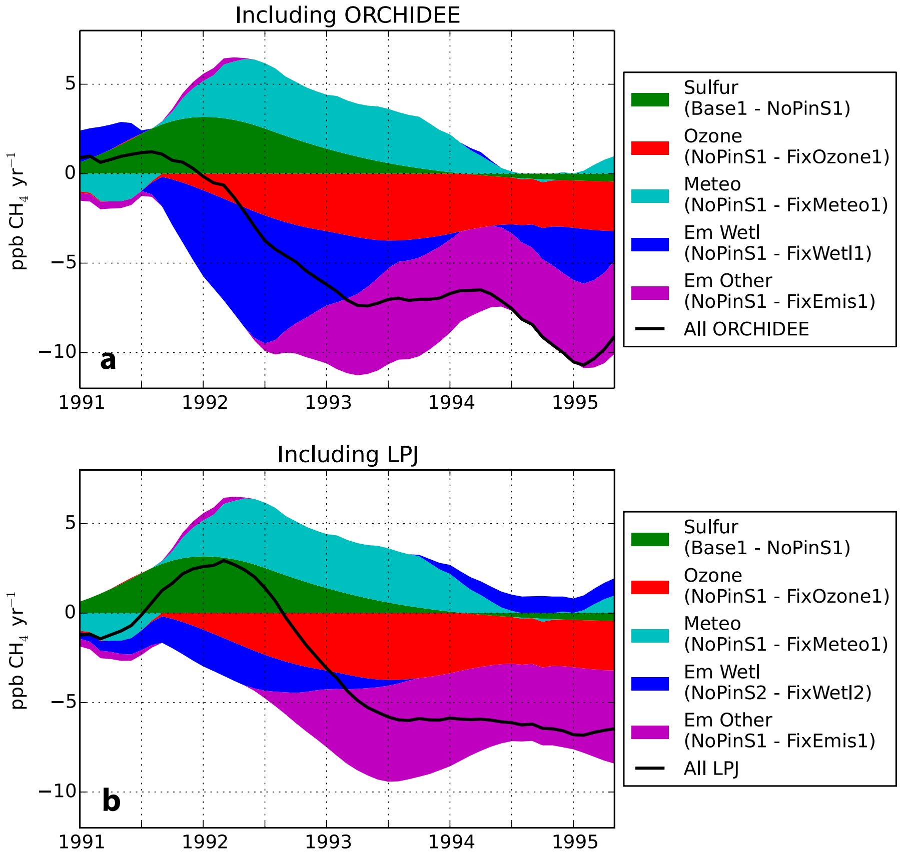

Figure 3. Global CH_4 growth rate variations with respect to the year 1990 induced by the different drivers, using a) ORCHIDEE and b) LPJ to represent variability in CH_4 emissions from wetlands. Simuluations from Set I are used in both plots to infer the effect of stratospheric sulfur, stratospheric ozone, meteorology and emissions other than wetlands. Simulations from Set II are used only to infer the effect of LPJ emission variability. The overall variability (‘All’) is calculated as the sum of the individual variations.

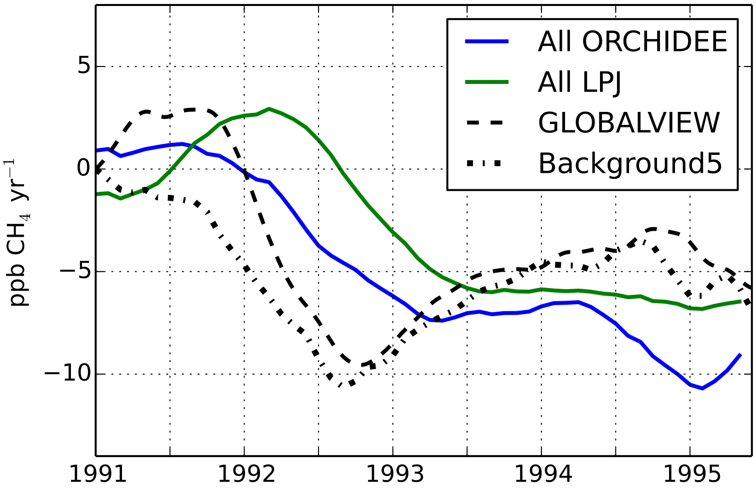

Figure 4. The explained CH_4 growth rate variability in the model using two wetland CH_4 emission inventories, and global deseasonalised CH_4 growth rate differences with respect to 1990 from the GLOBALVIEW observations, and from observations at 5 background stations.

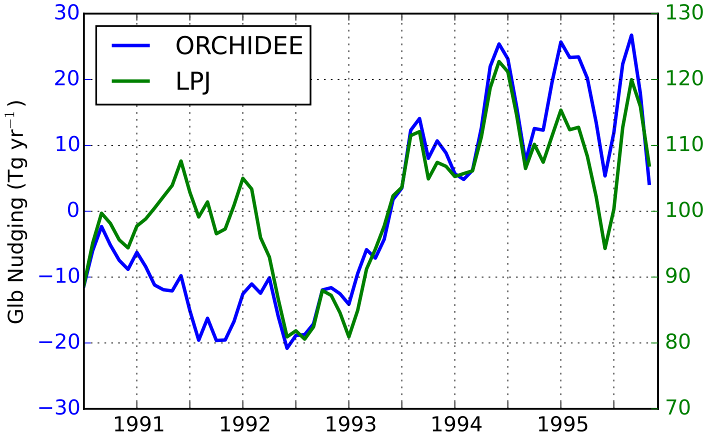

Figure 5. Global deseasonalised CH_4 nudging term for the ‘Base1’ (left y-axis) and ‘Base2’ (right y-axis) simulations, using CH_4 wetland emissions from ORCHIDEE and LPJ, respectively.

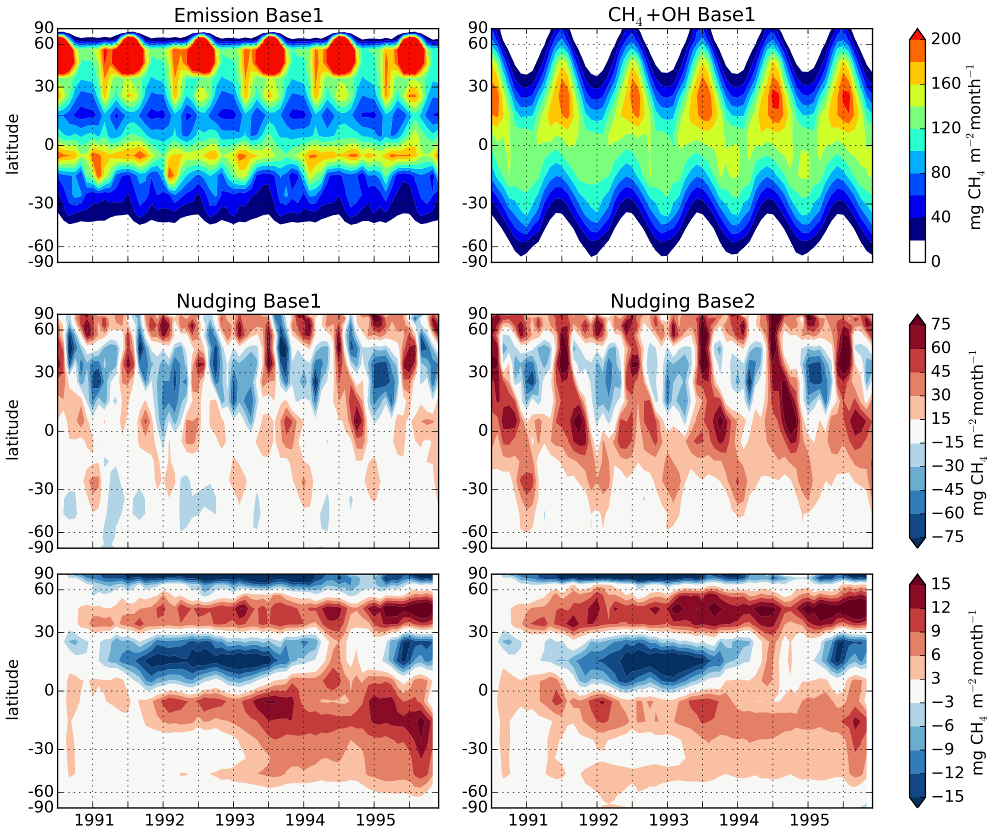

Figure 6. Zonal mean CH$_4$ a) emission and b) sink by reaction with OH in the ‘Base1’ simulation, zonal mean CH$_4$ nudging term when using CH$_4$ wetland emissions from c) ORCHIDEE (‘Base1’ simulation) and d) LPJ (‘Base2’ simulation), e and f) the deseasonalised nudging anomaly compared to 1990.

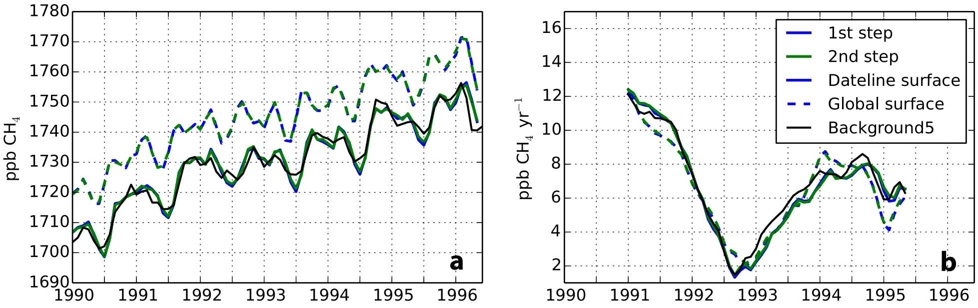

Figure 7. Surface mean CH_4 a) concentrations and b) growth rate for the two runs of 'Base1' simulation at the dateline (solid lines) and global mean (dashed lines). The black line shows the background mean concentrations based on 5 background stations.

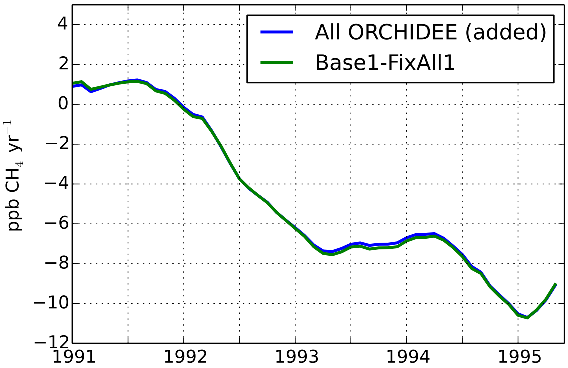

Figure 8. The combined effect of the 7 drivers of CH_4 variability on the global growth rate using ORCHIDEE emissions, assuming additivity (blue) and from the difference between 'Base1' and 'FixAll1'.